

PENETRABILITY OF CEMENT-BASED GROUTS DEPENDENT ON THE PSD-CURVE AND CEMENT CHEMISTRY

Almir Draganović
Conny Björk

PENETRABILITY OF CEMENT-BASED GROUTS DEPENDENT ON THE PSD-CURVE AND CEMENT CHEMISTRY

**Penetration av cementbaserade
injekteringsbruk beroende på kornkurva
och cementkemi**

Almir Draganović, KTH

Conny Björk, Nauplion AB

BeFo Report 134

Stockholm 2014

ISSN 1104 – 1773

ISRN BEFO-R—134—SE

Preface

The Scandinavian methodology for design and construction of tunnels and rock caverns depend on grouting to reduce water influx, and here cement grout is the dominating material. The demands of sealing traffic tunnels and tunnels in urban areas increase successively. With the development of finer cement particles in the grout mix, it is today possible to penetrate and seal fractures as thin as 70 μm . The grain size is very small in the fine material, and the smallest grain sizes cause problems due to flocculation and maybe also other chemical processes in the cement material. This reduces penetration into finer fractures than 70 μm , which generated research of the function of fine material and its impact on the grouting result.

Large efforts are made in the underground construction projects in rock to handle ingress of water and this is a time consuming and costly process to handle. Research that leads to a better result within this field is therefore important and a good reason to continue to support these efforts.

This research project studies mechanisms why the fine-ground cement is not penetrating the finer fractures. Research shows that the ability for the cement material to penetrate is not only based on amount of fine particles, but is more complex since also the chemical components are important.

A project group consisting of Almir Draganović (KTH) och Conny Björk (Nauplion AB) carried out the work. A reference group assisted the project group with valuable support and consisted of Håkan Stille (KTH), Pernilla Amsköld fd Petersen (Sika Sverige), Pentti Koski (Cementa) and Per Tengborg (BeFo). The project work was financed by Rock Engineering Research Foundation (BeFo) while Nauplion AB and Sicomant AB are part financier of a new cement milling machine.

Stockholm in October 2014

Per Tengborg

Förord

Den skandinaviska bergbyggnadstekniken bygger på att tunnlar och bergtrum tätas genom injektering, där cement är det helt dominerande materialet. Kraven på tätning av trafiktunnlar och tunnlar i tätbebyggda områden ökar successivt. Med de finmalda cementbruk som har utvecklats är det idag möjligt att täta sprickor ner till 70 μm . Man har mycket liten kornstorlek i finmaterialet, och de minsta partiklarna har visat sig skapa problem genom flockning och kanske andra kemiska processer. Dessa hindrar inträngning i finare sprickor än 70 μm , vilket gett upphov till att studera finmaterialets funktion och dess betydelse för injekteringsresultatet.

Stora insatser görs i berganläggningsprojekten under jord för att hantera vatteninträngning till anläggningarna och det är både en tids- och kostnadskrävande process. Forskning som kan ge ett bättre resultat inom detta område är därför viktig och en anledning till att fortsatt satsa inom området.

Detta forskningsprojekt studerar mekanismerna till varför finmalda cement inte tränger in i de finaste sprickorna. Forskningen visar att penetrationsförmågan inte enbart har med mängden finpartiklar att göra utan är mer komplex än så eftersom den tyder på att de kemiska beståndsdelarna är av betydelse.

En projektgrupp bestående av Almir Draganović (KTH) och Conny Björk (Nauplion AB) genomförde arbetet. Den referensgrupp som bistått projektgruppen och bidragit med värdefullt stöd har bestått av Håkan Stille (KTH), Pernilla Amsköld fd Petersen (Sika Sverige), Pentti Koski (Cementa) och Per Tengborg (BeFo). Projektarbetet finansierades av Stiftelsen Bergteknisk Forskning (BeFo) medan Nauplion AB och Sicomant AB delfinansierar tillverkning av en ny cementkvarn.

Stockholm i oktober 2014

Per Tengborg

Summary

Milling of cement is a method used to improve the penetrability of a grout. Earlier research has shown that cement can be milled to a certain grain size to improve penetrability. Further milling has a negative impact on penetrability, probably due to a larger proportion of finer particles.

Tests with INJ30, UF12 and T-cements confirm that grouts based on cement with a d_{95} of $30 \mu\text{m}$ has a better penetrability than grouts based on cement with a d_{95} of $12 \mu\text{m}$. The tests indicate that the reason for lower penetrability of fine-ground cement could also be related to the content of gypsum in the cement or other chemical components in the cement and not just the amount of fine particles.

Tests with SP-cements showed that penetrability of grouts based on fine-milled cement could be improved further. Developed SP-cement could be used to grout $50 \mu\text{m}$ fractures or even smaller. The study does not show clearly whether it is the reduction of fine particles or a changed chemical component of the cement that improved penetrability. In further tests, in addition to developing the milling process in controlling of the PSD curve, detailed chemical analyses of these cements are needed to clarify what the main reason for improved penetrability is.

Sammanfattning

Malning av cement är en metod som används för att förbättra inträngning av ett cementbaserat injekteringsbruk. Tidigare forskning visade att cement kan malas till en viss kornstorlek för att förbättra penetration. Fortsatt malning hade en negativ påverkan på penetrationen förmodligen på grund av en större andel av fina partiklar.

Försök med INJ30, UF12 och T-cement bekräftade att bruk baserade på cement med d_{95} lika med $30 \mu\text{m}$ har en bättre penetrationsegenskap än bruk baserade på cement med d_{95} lika med $12 \mu\text{m}$. Försöken indikerar att anledningen att bruk baserade på finmalda cement har en lägre penetration kan också vara relaterad till innehåll av gips i cement eller andra kemiska komponenter i cement och inte bara till andel av fina partiklar.

Försök med SP-cement visade att penetration av bruk baserade på finmalda cement kan ytterligare förbättras. Framtagen SP-cement kan användas till injektering av $50 \mu\text{m}$ sprickor eller ännu mindre. Studien visade inte klart om det är reducerat andel fina partiklar eller ändring i den kemiska sammansättningen av cement som har bidragit mest till en bättre penetration. Utöver utvecklingen av malningsprocessen med kontroll av kornkurvan behövs fortsatt forskning med detaljerad kemisk analys av provad cement för att klargöra vad huvudanledningen för förbättrad penetration är.

Contents

| | |
|--|----|
| 1. Introduction | 1 |
| 1.1. Milling of cement as a method to improve penetrability of cement-based grouts | 1 |
| 1.2. Phenomena or processes which can deteriorate penetration of cement grouts | 2 |
| 1.3. The aim of the study | 5 |
| 1.4. Organization of the report | 5 |
| 2. Measuring methods used in investigation | 7 |
| 2.1. Methods used to estimate particle size distribution (PSD) curves of cements: Malvern Mastersizer S, Malvern Mastersizer 3000, and Malvern Morphologi G3 | 7 |
| 2.2. Penetrability testing method, short slot | 8 |
| 2.3. XRD analysis technique | 10 |
| 2.4. SEM analysis technique | 11 |
| 3. Measurements with INJ30 and UF12 | 13 |
| 3.1. Introduction | 13 |
| 3.2. Manufacturing process of INJ30 and UF12 at Cementa Degerhamn | 13 |
| 3.3. Content of gypsum and C ₃ A in INJ30, UF12, and modified UF12 | 14 |
| 3.4. PSD curves of UF12 and INJ30 | 15 |
| 3.3.1. PSD curves of UF12 and INJ30 measured in alcohol | 15 |
| 3.3.2. Measured PSD curves of UF12 and INJ30 with the Malvern Mastersizer 3000 in air, alcohol, and water | 16 |
| 3.3.3. PSD curves of UF12, INJ30 measured with the Malvern Morphologi G3 | 18 |
| 3.3.4. Summarized measurements of PSD curves with the presented methods | 24 |
| 3.5. Penetration test, choice of grout recipe, and mixing method | 24 |
| 3.6. Results of penetrability measurements of UF12 and INJ30 based grouts | 25 |
| 3.7. SEM analysis of filter cake of UF12 and INJ30 grout | 28 |
| 3.8. Discussion of measurements with INJ30 and UF12 | 38 |
| 4. Measurements with T-cements | 39 |
| 4.1. Introduction | 39 |
| 4.2. Manufacturing of T cements | 39 |
| 4.3. Measured PSD curves of specially produced T-cements | 39 |
| 4.4. Performed penetrability measurements with T-cements | 41 |
| 4.5. Results of penetrability measurements of grouts based on T-cement | 41 |
| 4.6. Discussion of measurements with T-cements | 42 |
| 5. Measurements with SP-cements | 43 |
| 5.1. Introduction | 43 |
| 5.2. Manufacture of SP-cements | 43 |
| 5.3. Measured PSD curves of specially produced SP-cement | 43 |

| | | |
|------|---|----|
| 5.4. | Performed penetrability measurements with SP-cements | 45 |
| 5.5. | Results of penetrability measurements of grouts based on SP-cements | 45 |
| 5.6. | Discussion of measurements with SP-cements | 46 |
| 6. | Discussion | 47 |
| 7. | Conclusions | 48 |
| 8. | References | 49 |

1. Introduction

1.1. Milling of cement as a method to improve penetrability of cement-based grouts

Milling of cement is a method used to develop a grout which can seal very small fractures. Research has shown that cement can be milled to a certain grain size to improve the penetrability of the grouts. Further milling has a negative impact on penetrability due to a larger proportion of finer particles. These particles have a higher degree of hydration and flocculation and build flocks that stop penetration (Eklund and Stille, 2008; Draganović and Stille, 2011; Pantazopoulos et al., 2012).

Zingg et al. 2008 also studied flocculation and dispersion of cement pastes. Figure 1 shows images of a non-dispersed (left) and dispersed (right) cement paste sample. The cement paste samples are a mixture of ordinary Portland cement (OPC) and water with $w/c = 0.5$. In non-dispersed cement, small particles agglomerate and build a chain and agglomerate with larger particles. In dispersed samples, numerous small particles can be seen. These are dispersed using dispersion admixture. A conceptual model is also shown in the figure. This conceptual model illustrates the fact that the small particles play an important role in flocculation of cement particles. Reducing the amount of small particles will decrease the flocculation ability of cement pastes.

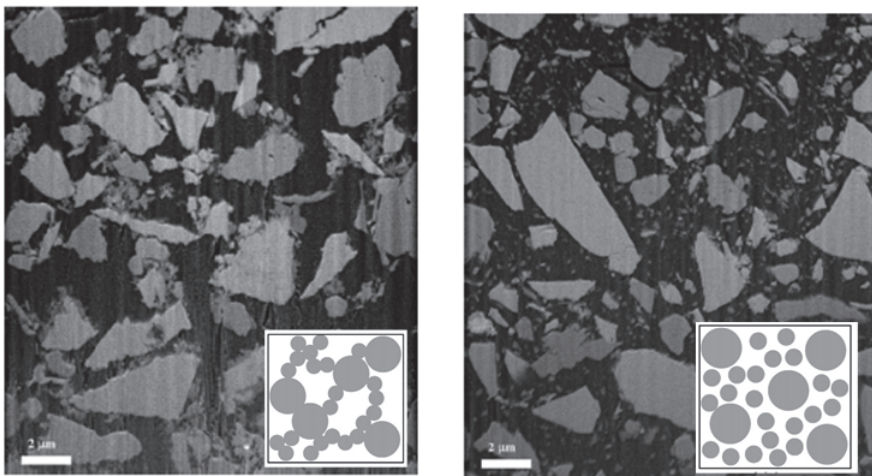


Figure 1: Cryo-FIB image of (left) non-dispersed cement paste after 24 minutes' hydration and (right) dispersed sample with dispersion admixture after 6 minutes' hydration. Zingg et al. 2008.

To describe cement with a number, some characteristic particle diameter is normally used. For example, a d_{95} of $30 \mu\text{m}$ means that in 95% of the cement weight or volume the particle diameter is below $30 \mu\text{m}$. Penetrability of a grout also needs to be described. Parameters b_{critical} and b_{min} are a way to describe the penetrability of a grout. Grout can penetrate apertures larger

than b_{critical} without any filtration or plug formation. Grout cannot penetrate apertures smaller than b_{min} at all. At apertures between b_{min} and b_{critical} , grouts are filtered and a plug forms (Eriksson and Stille, 2003).

Draganović and Stille (2011) showed that grout based on INJ30 cement with a d_{95} of $30 \mu\text{m}$ has a better penetrability than grout based on UF12 cement, which is finer milled cement with a d_{95} of $12 \mu\text{m}$. Grout based on INJ30 cement has a b_{critical} of around $65 \mu\text{m}$ measured with a short slot. Grout based on UF12 cement has a b_{critical} of around $250 \mu\text{m}$. Eklund and Stille (2008) showed a similar result. Parameter b_{critical} begins to increase when d_{95} decreases approximately below $20 \mu\text{m}$. Pantazopoulos et al. (2012) tested the penetrability of grouts based on cements with a d_{100} of 100, 40, 20 and $10 \mu\text{m}$. Penetrability was tested by grouting a sand column filled with sand of different gradations. The results showed that grouts based on cement with a d_{100} of $40 \mu\text{m}$ had the best penetrability. This confirms the finding that uncontrolled further milling after a certain grain size causes penetrability to deteriorate.

1.2. Phenomena or processes which can deteriorate penetration of cement grouts

There may be different reasons why grouts based on cement with a d_{95} of around $30 \mu\text{m}$ have better penetrability than grouts based on cements with a d_{95} of around $12 \mu\text{m}$. **Flocculation** is one. Finer ground cements have larger amounts of fine particles, which have a larger affinity to flocculation than more coarsely ground cements. The finer particles also contribute to flocculation of larger particles, as illustrated in Figure 1.

Presence of **free aluminate** (C_3A) in cement might also deteriorate the penetrability of a grout. Tricalcium aluminate, C_3A , is a clinker mineral in Portland cement with high reactivity. C_3A will immediately hydrate in contact with water in case of no or very low availability of sulfate in solution, Ramachandran et al. (1998). The instant hydration of these particles is known as “flash setting”. See case IV in Figure 2. Flash setting occurs during the first 10 minutes of hydration. Flash setting will deteriorate the penetrability of a cement grout. Finer ground cements can contain a larger amount of free C_3A than coarsely ground cements even if they are produced from the same cement. Figure 3 illustrates cement particles with C_3A at the center of the particles. Further grinding of the particles can free enclosed C_3A .

| Reactivity of C_3A in Clinker | Availability of sulfate in solution | Hydration Age | | | |
|---------------------------------|-------------------------------------|---------------|-------------------|--|-------------------------|
| | | < 10 min | 10 - 45 min | 1 - 2 hours | 2 - 4 hours |
| Low | Low | workable | workable | less workable | normal set |
| High | High | workable | less workable | normal set | Ettringite in pores |
| High | Low | workable | quick set | | |
| High | None or very low | flash set | | C_4AH_{13} and C_4ASH_{13} in pores | |
| Low | High | false set | | Crystallization of gypsum needles in pores | |

Figure 2: Schematic illustration of possible phenomena in cement paste as a function of the $C_3A:CaSO_4$ ratio and time. Ramachandran et al. (1998).

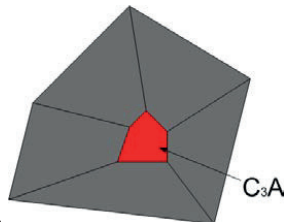


Figure 3: A cement clinker mineral

One of the functions of gypsum in cement is to prevent fast hydration of C_3A . A low amount of C_3A and high availability of sulfate in solution can cause a “false setting” of cement pastes. See the illustration of this phenomenon in Figure 2, Case V. “False setting” is caused by **crystallization of gypsum needles** in cement pores. This might also deteriorate the penetrability of a cement grout. It is therefore important to use cement with a low amount of C_3A and a proper amount of gypsum. Figure 4 illustrates this phenomenon. The figure shows two pictures from an analysis of a white Portland cement (CEM I) from Aalborg in Denmark (Gandolfi et al. 2010). The pictures show elongated needle-like ettringite crystals after 10 minutes of hydration. Ettringite is a product of a chemical reaction between aluminate or ferrite and gypsum in cement. White Portland cement is in principle the same as ordinary Portland cement except for the presence of some oxides related to coloring. According to the producer’s data sheet, this cement contains less than 5% C_3A , 1% C_4AF and 1.8-2.3% sulfate (SO_3). Anlåggningscement has a similar chemical content except for a somewhat lower content of C_3A . It contains 1.5-2.5% C_3A . Anlåggningscement also contains somewhat more SO_3 , 2.3-2.5%. The pictures shown in Figure 4 were taken with an Environmental Scanning Electron Microscope (ESEM). With an ESEM, a specimen can be examined in any gaseous condition and both wet or dry.

Ettringite formation during hydration can also influence penetration. Figure 5 shows ettringite and hydration products of OPC after 6 minutes' hydration taken with a Cryo-SEM. It can be seen that ettringite is in a range of 200 nm. Ettringite and hydration products in this system should not influence the penetration of grout as much as the hydration products in the system presented in Figure 4.

It is necessary to test if ettringite or gypsum formation could influence penetration in Anlæggingscement or INJ30 and UF12, which are produced from this cement.

Oversized particles in cement might also deteriorate penetration.

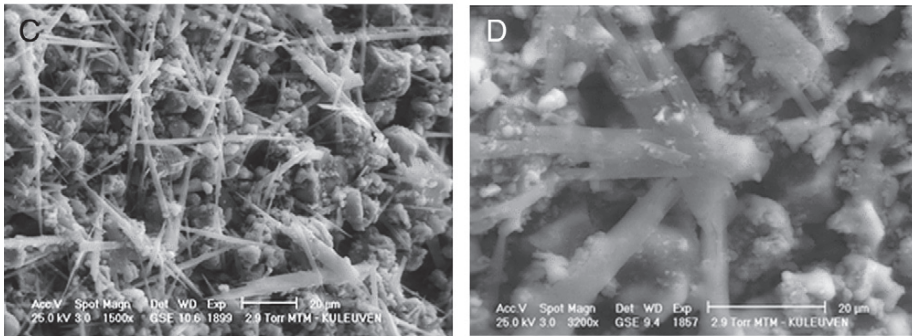


Figure 4: ESEM-EDX analysis of freshly prepared cement paste after 10 minutes of hydration. Elongated needle-like ettringite crystals. The cement used is white Portland cement, which contains 1.8-2.3 SO₃ according to the product description. (CEM I, Aalborg, Denmark). From Gandolfi et al. 2010.

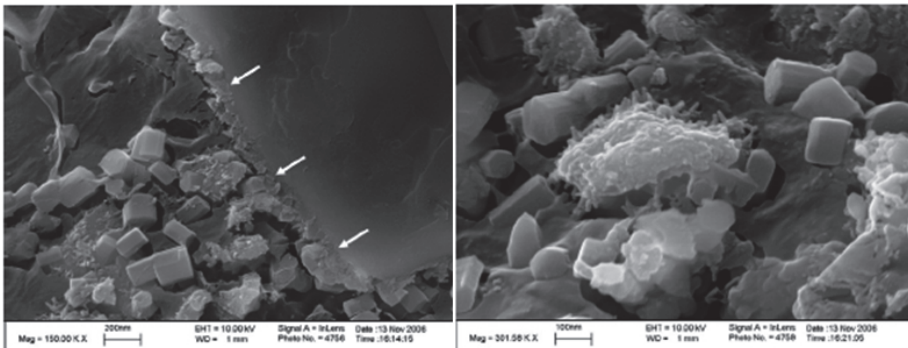


Figure 5: (Left) Cryo-SEM image of sample dispersed and hydrated for 6 minutes showing crystals of ettringite in pore solution and hydration products (white arrows) on the surface of clinker mineral. Bar = 200 nm. (Right) Cryo-SEM image of sample after 6 minutes of hydration showing some hydration products covering hexagonal ettringite. Bar = 100 nm.

1.3. The aim of the study

The aim of this study is to investigate how reduction of the proportion of fine particles in cements influences penetrability of cement-based grouts. The study also aims to make a preliminary investigation related to other reasons such as presence of free aluminate (C_3A) in cement, e.g. crystallization of gypsum or ettringite or oversized particles, which might deteriorate the penetrability of a grout.

1.4. Organization of the report

In the study, cements INJ30 with a d_{95} of 30 μm and UF12 with a d_{95} of 12 μm were chosen to study penetrability of grouts based on relatively coarser and finer ground cements. How the amount of fine particles influences penetration is further tested with T-cements. T-cements are cements with fewer fine particles than UF12 and are produced from INJ30 and UF12. The chemistry of this cement is the same as or similar to UF12. Preliminary measurements with SP-cements, i.e. finely ground cement but produced from other Portland cements, are also performed to test if cement chemistry, besides the PSD curve, is also important for penetration.

The PSD curves of the tested cements were measured with different instruments to reduce uncertainty in the measured PSD curves. Some of these instruments are also used to investigate flocculation of the cements and presence of oversized particles.

The penetrability of the grouts based on these cements was tested with short slots. The sizes of the slots are control-measured to reduce uncertainty regarding their size.

The size and shape of cement particles, presence of oversized particles and possible crystallization of gypsum or ettringite needles in cement were investigated by means of SEM analysis of the filter cake.

XRD analysis was performed to investigate the presence of C_3A and gypsum in unhydrated cements and ettringite and crystallization of gypsum in hydrated cement paste.

2. Measuring methods used in investigation

2.1. Methods used to estimate particle size distribution (PSD) curves of cements: Malvern Mastersizer S, Malvern Mastersizer 3000, and Malvern Morphologi G3

The Mastersizer S is an older instrument while the Mastersizer 3000 is the latest model from Malvern and can measure the PSD curve of a material in air, alcohol or water. In measurement in air, a small amount of a material, a few grams only, is placed in the instrument. This material is spread in an air flow through a pipe under 150 kPa (1.5 bar) pressure. The material is dispersed due to different velocity gradients and collisions between particles and particle-to-wall collisions, as illustrated in Figure 6. During the flow, the particles are illuminated with light from a laser. The PSD curves are estimated by measuring angular variation of light scattered from a laser beam which passes through dispersed samples. Material can also be dispersed in alcohol or water and measurements performed in a similar way. Comparing the curves measured in air, alcohol and water, the flocculation ability of the cement particles in these three different media can be also studied. Differences between these PSD curves indicate flocculation. The reduced amount of fine particles and the higher amount of coarser and larger particles indicate that some of the fine particles have flocculated with coarser or other fine particles.

The Morphologi G3 is also an instrument from Malvern which can be used to measure PSD curves. This is a static method. Material is dispersed before measurement and then placed on a glass disc and illuminated from the top and/or bottom. See Figure 7. Material can be dispersed in air and analyzed dry or in other media such as water or alcohol and then placed on the glass disc.

In this study, cement was analyzed dry and suspended in water. The dispersion process of dry material can be seen in this video: <http://www.youtube.com/watch?v=FU-Rx0Kjf3c>. In analysis of suspended material in water, a small amount of cement is placed in water and mixed by hand. A few drops of suspension are then placed on a glass disc with a pipette and covered with another glass disc.

The result of a measurement is a picture of every individual particle. The PSD of the sample is determined by means of picture analysis. A great advantage of this method compared to the Mastersizer 3000 is the possibility to see if a large particle is one single particle or an assemblage of smaller particles. Any presence of oversized particle or particle flocks measured with the Mastersizer 3000 can be verified with the Morphologi G3.

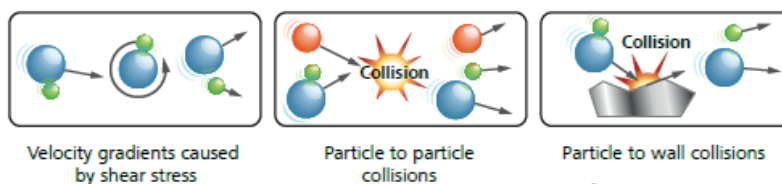


Figure 6: Dispersion of particles in air flow in a Malvern Mastersizer 3000



Figure 7: Measurement with a Malvern Morphologi G3

2.2. Penetrability testing method, short slot

The penetrability of grouts was in this study tested with a short slot in the laboratory. Figure 8 shows the equipment. Assembled discs give a slot with a constriction at both ends. Grout is poured into a container and pressed out through a slot using compressed nitrogen. The weight of the grout with container is measured at the same time. The grouting pressure was 1.78 MPa (17.8 bar) and the volume of the grout container used in the tests was 2.752 l. A detailed description of the measurements can be found in Draganović and Stille (2011).

To minimize uncertainty about the size of the slots used in these measurements, a control measurement of the 50, 30, and 20 μm slots was made by Hexagon Metrology Nordic AB in Gothenburg. The control measurements were made with a DEA Global model 153314 with an accuracy of $\pm 1.5 \mu\text{m}$. The control measurements were made on two sections on each side of the slot. Section A-A is located 5 mm from the constriction and section B-B 2 mm. Three measuring points on each section are located in the center of the slot and close to its edges. The results are shown in Figure 9, Figure 10 and Figure 11. As can be seen from the figures, the sizes of the measured slots are somewhat larger than those given by the manufacturer. The results of the control measurements of the slots are also shown in Table 1. Based on the results from the control measurements, the 50 μm slot will be called a 70 μm slot, the 30 μm slot a 50 μm slot and the 20 μm slot a 30 μm slot.

It is also important to bear in mind that the plates are not ideal plates and that skewness of the plates might cause the openings of the slots to be somewhat larger than those shown in Table 1.

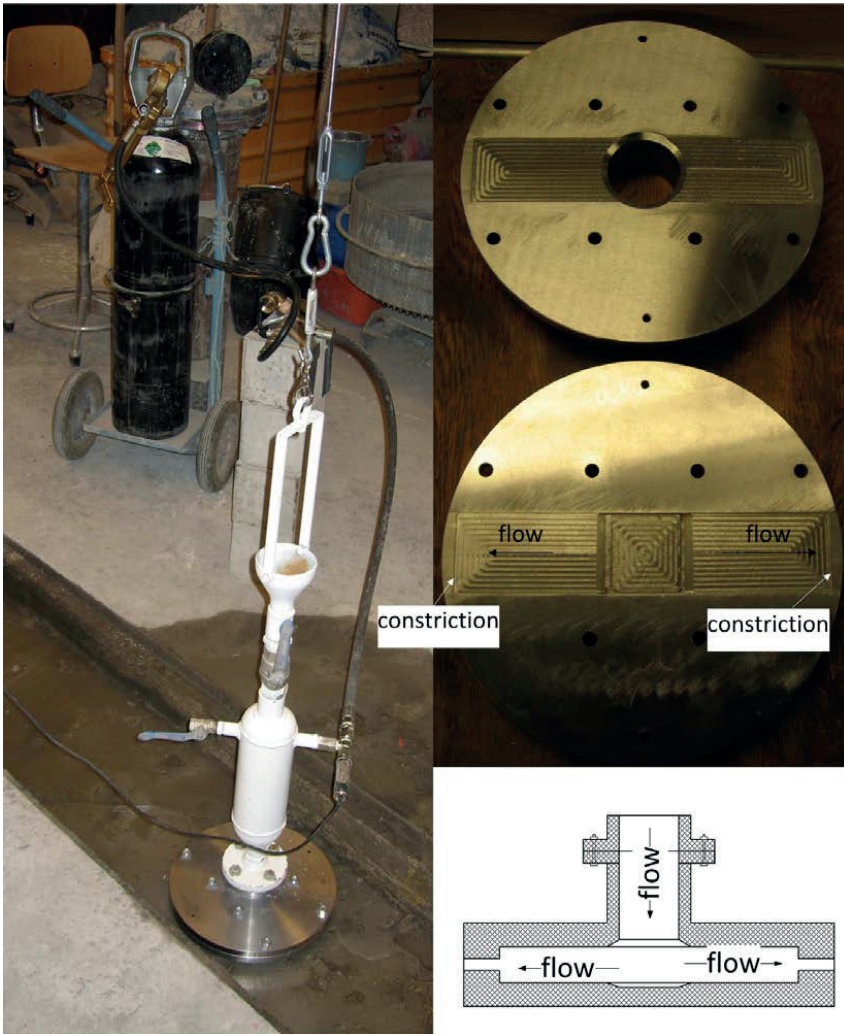


Figure 8: Short slot

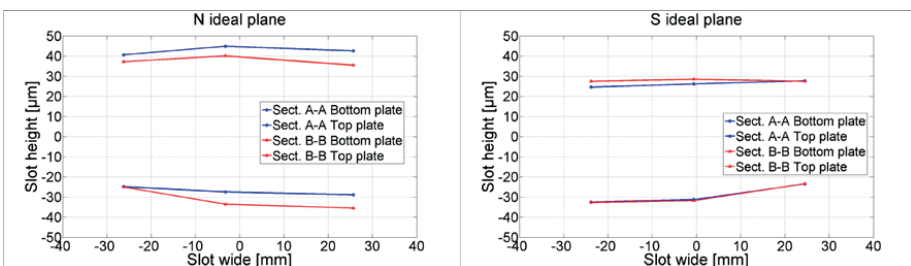


Figure 9: 50 μm slot. Measured section A-A is 5 mm from the constriction and section B-B 2 mm from the constriction.

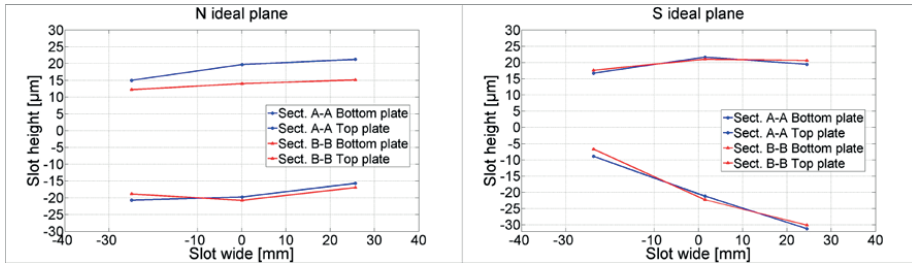


Figure 10: 30 μm slot. Measured section A-A is 5 mm from the constriction and section B-B 2 mm from the constriction.

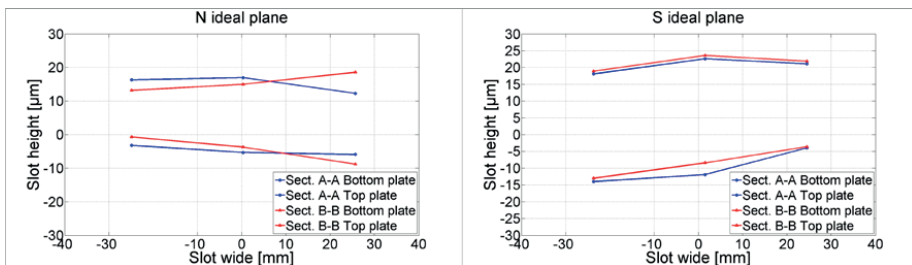


Figure 11: 20 μm slot. Measured section A-A is 5 mm from the constriction and section B-B 2 mm from the constriction

Table 1: Control measurements of 50 μm , 30 μm , and 20 μm slots

| | 50 μm slot | 30 μm slot | 20 μm slot |
|--------------------------|-----------------------|-----------------------|-----------------------|
| N side (μm) | 69 | 35 | 20 |
| S side (μm) | 56 | 50 | 30 |

2.3. XRD analysis technique

X-ray diffraction (XRD) is a technique suitable for studying crystalline materials such as clinker material and hydration products in a cement paste, Scrivener et al. (2004). The X-ray diffraction pattern is unique for each crystalline material. The results of one measurement are presented in a 2 θ -axis (x-axis) versus intensity number diagram (y-axis). The position of the peaks on the 2 θ axis is related to the kind of crystal and the intensity of the peak to the amount of crystalline material in the sample. A higher amount of material in a sample gives a higher peak. Figure 12 illustrates the measuring principle in this method and a result of a measurement.

An analysis of INJ30, UF12, and modified UF12 was made regarding the presence of gypsum, C₃A, crystallization of gypsum, and formation of ettringite.

Measurements were performed with both dry cement and suspended in water. Modified UF12 is UF12 where the amount of fine particles is reduced as in T cements. INJ30, UF12, and modified UF12 are mixed with water with a w/c ratio of 1.0. Hydration was stopped after 30 minutes by

adding methanol to the sample. The sample was then mixed again and dried at 40°C for approximately 18 hours before analysis.

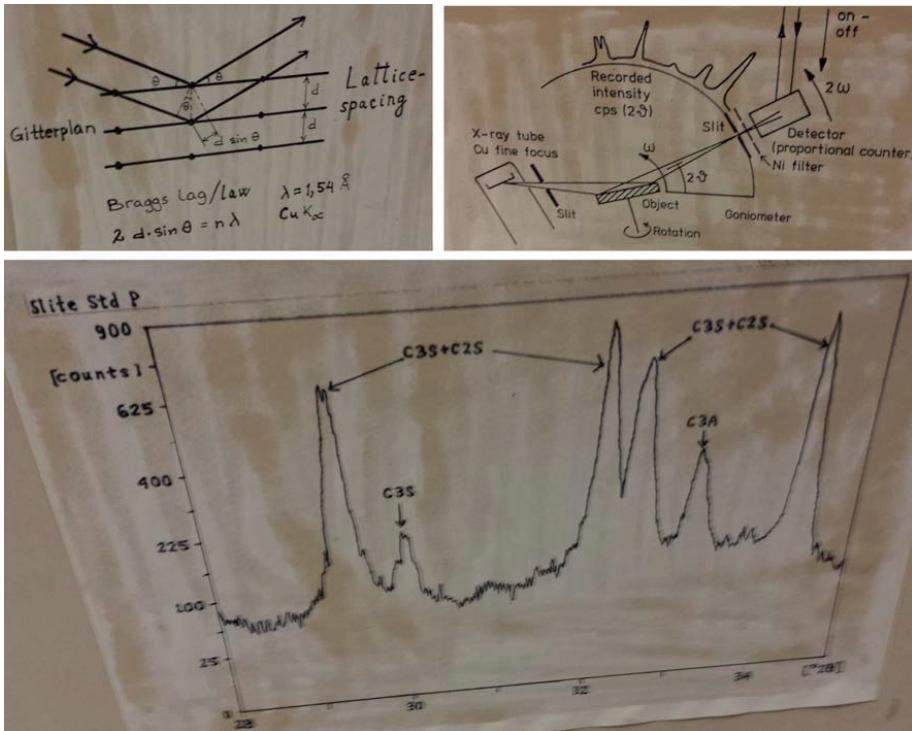


Figure 12: Illustration of XRD measuring method and a result of a measurement.

2.4. SEM analysis technique

A scanning electron microscope (SEM) produces an image of a sample by scanning it with a focused beam of electrons. The electrons interact with atoms in the sample and produce many different signals. These signals are used to create an image and also for chemical analysis of the samples. The method can be used to investigate the size and shape of cement particles and the presence of oversized particles.

The pictures shown in Figure 4 were taken with an Environmental Scanning Electron Microscope (ESEM). A specimen can be examined in an ESEM in any gaseous state and both wet or dry. It is a great advantage compared to SEM, where the sample has to be dried and placed in a vacuum, which might affect the sample. The size of the needle-shaped ettringite particles shown in Figure 4 was in the range of 20-30 μm . It is debatable if these needle-shaped particles can also be observed with an SEM due to the sample being dried. These needle-shaped particles can be broken.

3. Measurements with INJ30 and UF12

3.1. Introduction

In this study, INJ30 with a d_{95} of 30 μm and UF12 with a d_{95} of 12 μm were chosen as cements to represent relatively coarser and finer ground cements. These cements were also used in some earlier studies. If the results confirm the results from the previous studies, this will reduce uncertainty in measuring errors and confirm that the penetrability problem is related to cement.

It is therefore also important to investigate similarities and differences between these cements, not just related to the PSD curve but also chemical content which might influence the penetrability of grouts produced from them. It is of particular interest to investigate if there are any differences in the production process regarding C_3A and gypsum content or some other differences in chemical content.

3.2. Manufacturing process of INJ30 and UF12 at Cementa Degerhamn

INJ30 and UF12 are two fine-ground cements produced by Cementa for grouting purposes. Both are produced from Anl ggningscement (ANL). ANL cement is Portland cement CEM I 42,5 N –SR 3 MN/LA. Detailed information about this cement can be found in Appendix 1. According to the manufacturer, ANL cement contains 4% gypsum, which is added to the cement during grinding of clinker. ANL cement has a low content of tricalcium aluminate (C_3A), which can vary between 1.5 to 2.5%.

Figure 13 illustrates the manufacturing process of INJ30 and UF12 cements at the factory in Degerhamn. ANL cement is blown into a wind sieve, where particles are separated. Particles smaller than a particular size are stirred out as final product INJ30 or UF12, while larger particles continue to a grinder and are milled and sieved again. This is a continuous process which is stopped when the desired amount of cement has been produced. ANL cement already contains 4% gypsum and a further 0.2% is added during grinding and sieving. According to the manufacturing process, INJ30 and UF12 should have the same chemical composition.

INJ30 and UF12 are ground in a vertical ball mill where cement particles are ground through attrition with mill elements while passing the mill. Mill elements are produced from hard metals and have a cylindrical shape with a height of 8 mm and diameter of 8 mm. See Figure 13 b). Because of friction between mill elements themselves and between mill elements with cement, heat develops in the mill. According to the manufacturer, the temperature in the mill where INJ30 is produced is below 130°C but in the mills where UF12 is milled the temperature is around 250°C. At temperatures higher than 130°C, gypsum can change from dihydrate ($\text{CaSO}_4 \cdot 2\text{H}_2\text{O}$) to hemihydrate ($\text{CaSO}_4 \cdot 0.5\text{H}_2\text{O}$). Hemihydrates are more soluble in water than dihydrate (Betonghandbok, 1994). Due to the higher temperature in the milling process, UF12 may contain more soluble hemihydrates than INJ30. This difference may be important and the content of gypsum and C_3A in these cements is therefore also investigated by means of XRD analysis.

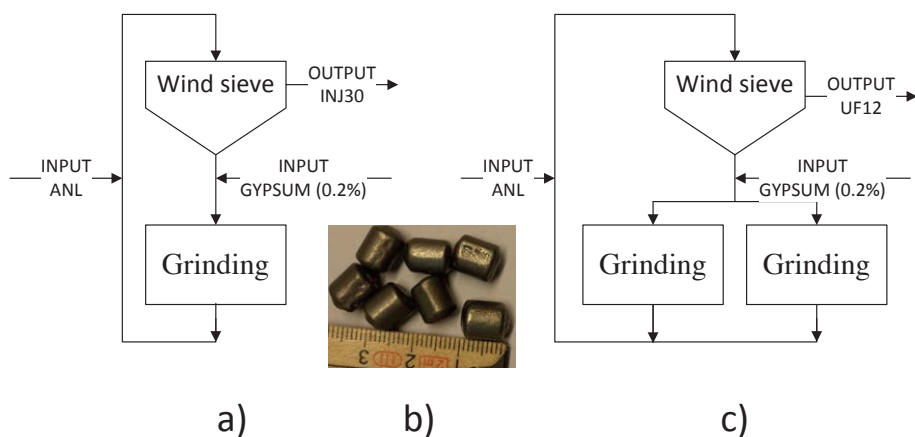


Figure 13: Manufacturing processes: a) INJ30, c) UF12 cement, and b) mill elements.

3.3. Content of gypsum and C₃A in INJ30, UF12, and modified UF12

The content of free C₃A and gypsum can influence the penetrability of a cement-based grout. The manufacturing process of INJ30 and UF12 shows that there is a possibility that UF12 may contain more hemihydrate than INJ30 due to heating of UF12 above 130°C during the grinding process. There is also a possibility that UF12 contains a larger amount of free C₃A than INJ30 due to finer grinding, even if the C₃A content of these cements is relatively low. A modified UF12 was also tested. A modified UF12 is cement produced from UF12, where the amount of fine particles has been reduced by sieving. This reduction can change the content of a cement if some component is not evenly spread in smaller and larger particles. This might occur if some material in the cement is easier to grind than others.

The results from XRD analysis of unhydrated INJ30, UF12, and modified UF12 and of hydrated cement pastes after 10 or 30 minutes are summarized in Table 2 and shown in Figure 39 and Figure 40 in Appendix 2. The values in Table 2 represent area under peaks from the “2θ intensity number” diagram for the respective component. See Figure 39 and Figure 40 in Appendix 2. It is a measure of the presence of a component in a material and can be used for relative comparison of analyzed material.

The analysis showed that unhydrated INJ30 contains gypsum (CaSO₄·2H₂O) and hemihydrate (CaSO₄·1/2 H₂O) in measurable amounts. The amount of gypsum increases in hydrated cement pastes after 10 and 30 minutes, while the amount of hemihydrate decreases. Hemihydrate is more soluble in water than gypsum, 0.7 g/l and 0.2 g/l respectively at 25°C. A decrease in hemihydrates and an increase in gypsum in hydrated cements could be the result of a secondary gypsum formation according to reaction:



This is a phenomenon which can occur in a Portland cement. This secondary gypsum is usually consumed over a period of 24 hours in reaction with other clinker materials.

UF12 and modified UF12 contain approximately the same amount of hemihydrate but a borderline measurable amount of gypsum. The reason could be heating of UF12 during manufacturing process. The amount of gypsum increases in hydrated cement pastes due to the reaction of

hemihydrate with water as described above, reaction (1).

According to the technical data sheet (Appendix 1), ANL cement can contain 1.5- 2.5% C₃A. The XRD analysis showed that the amount of C₃A was small in all three cements and is hardly measurable with this method. The presence of ettringite in hydrated cement pastes proves that C₃A exists in these cements. Ettringite is a product of a chemical reaction between C₃A and sulfates in cement pastes during early hydration. Ettringite formation is largest in UF12. UF12 has a higher amount of fine particles than INJ30 and modified UF12. This could mean that the amount of free C₃A in UF12 is somewhat higher than in the other two cements.

Formation of secondary gypsum and ettringite in all three cement pastes might influence penetrability due to possible agglomeration of cement particles. In particular the formation of secondary gypsum might be important if gypsum crystalizes in the form of needles. This is investigated using a SEM microscope. In SEM analysis, it is also possible to estimate the presence of oversized particles.

Table 2: XRD analysis of unhydrated INJ30, UF12, and Modified UF12 cement and hydrated cement paste after 10 and 30 min of hydration.

| Component | INJ30 unhydr. | INJ30 10 min hydr. | INJ30 30 min hydr. | UF12 unhydr. | UF12 30 min hydr. | Mod.UF12 unhydr. | Mod.UF12 30 min hydr. |
|--------------|---------------|--------------------|--------------------|--------------|-------------------|------------------|-----------------------|
| Gypsum | 10.25 | 17.73 | 14.84 | 4.03 | 11.43 | 1.51 | 13.31 |
| Hemi-hydrate | 13.76 | 5.87 | 7.92 | 12.83 | 5.34 | 14.16 | 5.69 |
| Ettringite | 0 | 15.08 | 14.61 | 0 | 19.65 | 0 | 15.33 |

3.4. PSD curves of UF12 and INJ30

3.3.1. PSD curves of UF12 and INJ30 measured in alcohol

The influence of the amount of fine particles in a cement on penetrability is the main issue in this study. The PSD curves of cement are therefore measured using different methods in different media to reduce uncertainty in the measurements.

UF12 is cement with a d₉₅ of 12 μm and INJ30 with 30 μm. Figure 14 shows the particle size distribution of these cements measured in alcohol using three different instruments, viz. the Cilas 850, the Malvern Mastersizer S, and the Malvern Mastersizer 3000. The PSD curves referred to as “before 2003 Cil. 850” were measured before 2003 with the Cilas 850. In 2003, the cement manufacturer changed to the Malvern Mastersizer S. The PSD curves measured with this instrument are different; in particular the amount of fine particles is much lower. The amount of particles smaller than 2 μm in UF12 was 40% measured with the Cilas 850 and just 20% with the Mastersizer S. This could mean that the dispersion process of particles in a sample during measurements is better in measurements with Mastersizer S.

To clarify this uncertainty, the PSD curves of these cements were also measured with the latest model from Malvern, the Mastersizer 3000. As can be seen from the measurements presented in Figure 14, the PSD curves from the Mastersizer S and the Mastersizer 3000 are similar. There are no differences between the PSD curves of INJ30 measured with these two instruments. The only measured difference is in the amount of fine particles smaller than 2 μm in UF12 cement. According to the Mastersizer 3000, UF12 has a lower amount of these particles compared to the Mastersizer S. Measurements of particles larger than 2μm in UF12 are quite similar.

According to these measurements, the parameter d_{95} of UF12 is also correct. 95% of particles are below 12 μm . In some measurements, the largest particles are up to 30 μm or even larger. These particles might decrease the penetrability of grout based on this cement.

Parameter d_{95} of INJ30 is 30 μm and according to these measurements almost 100% of particles are smaller than 30 μm .

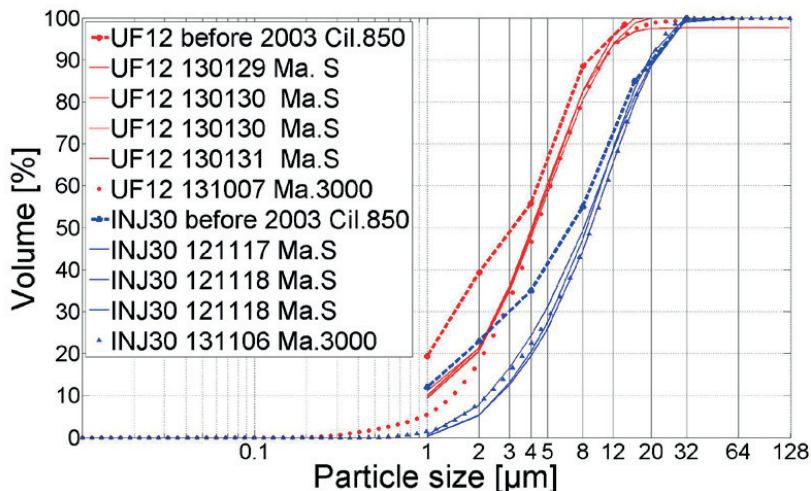


Figure 14: Particle size distribution of UF12 and INJ30 cement measured with the Cilas 850 before 2003, the Malvern Mastersizer S and the Malvern Mastersizer 3000 in alcohol.

3.3.2. Measured PSD curves of UF12 and INJ30 with the Malvern Mastersizer 3000 in air, alcohol, and water

Measurements of PSD curves in alcohol can underestimate the amount of fine particles in cement due to possible flocculation of fine particles with other particles or with themselves. PSD curves of INJ30 and UF12 are therefore also measured in air and water. These measurements are performed with the Mastersizer 3000 since this instrument can measure PSD curves continuously in air, isopropyl alcohol (IPA), and water. Figure 15 shows the PSD curves of INJ30 and UF12 estimated with this instrument. It can be seen that measurements in air show a larger amount of fine particles in both cements compared to measurements in alcohol and water. All particles less than 1 μm had flocculated in water and the majority of particles between 1 and 3 μm had also flocculated in both cements. This indicates that fine particles are flocculated and flocculation is greatest in water.

The size of the largest particles increased in UF12 both in alcohol and water. This means that these particles are also flocculated. The sizes of the largest particles in INJ30 were the same in both air and alcohol. This might indicate that the particles around 30 μm are easier to disperse. But in measurements in water these particles were also flocculated.

Figure 16 shows these measurements in time. In measurements in airflow, a stable curve is reached relatively fast for both INJ30 and UF12 cements and does not change during the

measurement time. In measurements in alcohol, INJ30 also reached a stable curve relatively quickly. Unlike in measurements in air and alcohol, in measurements in water, INJ30 and UF12 become increasingly coarser with time. This is a clear illustration of how cement particles during flowing in water flocculate with time. This could be important in agitation processes. It means that grout can also flocculate during agitation. Figure 17 shows D_{10} , D_{50} , and D_{90} in time during measurement in water. The largest changes are related to coarser particles. According to Figure 16, INJ30 and UF12 reached the same D_{100} of $50 \mu\text{m}$ in measurements in water. This might have a significant effect on the penetrability of cement. The effect of finer grinding of UF12 is eliminated by flocculation.

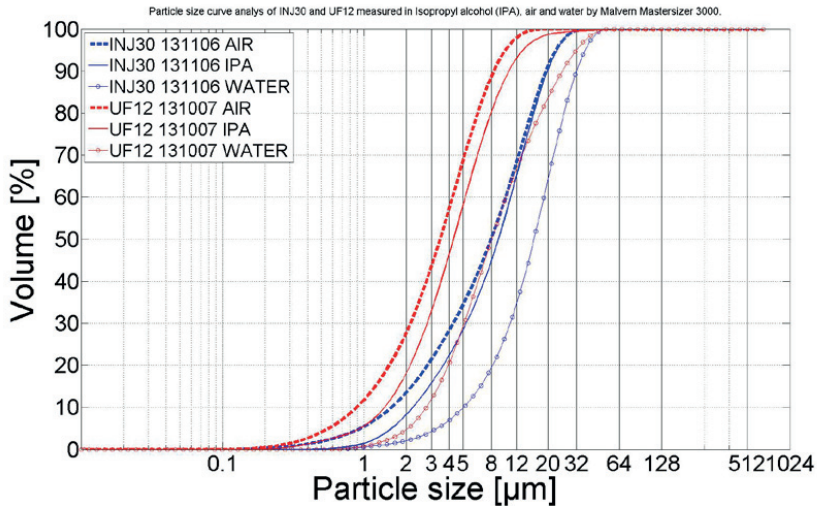


Figure 15: PSD curves of INJ30 and UF12 estimated with the Malvern Mastersizer 3000 in air, water, and isopropyl alcohol (IPA).

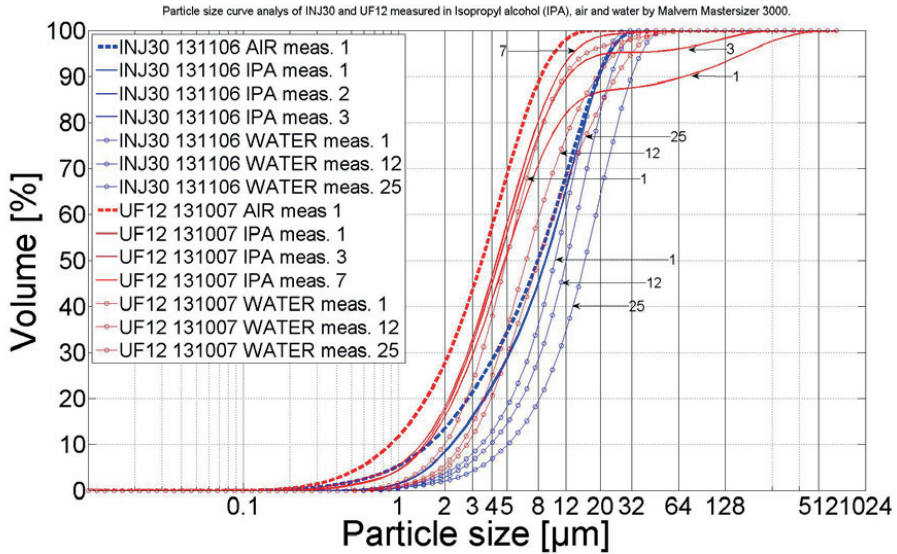


Figure 16: PSD curves shown in time until they reach a stable state from the measurements presented in Figure 16.

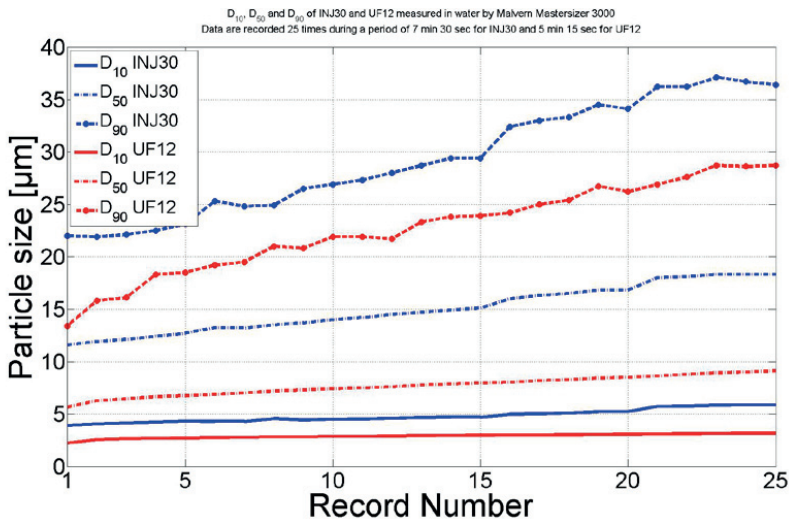


Figure 17: D_{10} , D_{50} , and D_{90} of INJ30 and UF12 measured in water for 7 minutes and 30 seconds and 5 minutes and 15 seconds

3.3.3. PSD curves of UF12, INJ30 measured with the Malvern Morphologi G3

The Malvern Morphologi G3 is an instrument which measures PSD curves by means of picture analysis. In this way, it is possible to see if the largest particles in a cement are oversized particles or flocks of smaller particles. Figure 18 shows the PSD curves of dry INJ30 and UF12 cement (AIR) and suspended in water measured with the Morphologi G3 and the Mastersizer 3000. The largest particle in dry INJ30 was around 27 μm while in water suspension the largest particle was around 41 μm . Figure 19 shows a picture analysis of this measurement. The

analysis showed that the largest particle in the dry sample was a particle of $27.6 \mu\text{m}$ and not a flock of several particles, while the “largest particle” in water suspension of $41.52 \mu\text{m}$ was an assemblage of several smaller particles.

This measurement with the G3 showed a very small amount of fine particles in INJ30. Figure 18 also shows the PSD curve of INJ30 measured in air with the Mastersizer 3000. It can be seen that the amount of largest particles is approximately the same in both measuring methods in air while the amount of fine particles is much higher when measured with the Mastersizer 3000. In measurements with the Morphologi G3, the D_{10} of dry INJ30 G3 is $4.82 \mu\text{m}$ (Table 3 or Figure 18) and $1.8 \mu\text{m}$ measured with the Mastersizer 3000. This means that the finest particles in the cement in measurements with the Morphologi G3 were not properly dispersed and are not detected.

Comparing the PSD curves of dry INJ30 and suspended in water measured with the G3, there is a large difference as regards presence of fine particles. The finest particles in water suspension are flocculated with larger particles and are not detected.

Measurements of UF12 showed similar results. It seems that UF12 was just better dispersed than INJ30. The PSD curves in Figure 18 show similar results between dry UF12 and suspended in water as regards largest particles and picture analysis confirmed this. Figure 21 shows a picture of UF12 analyzed with the Morphologi G3. It can be seen that UF12 contains particles of up to $22 \mu\text{m}$ and these are not assemblages of smaller particles.

The measurements with the Morphologi G3 showed that this instrument can be used for analysis of the presence of oversized particles and investigation of whether the largest particles are assemblages of smaller particles or individual particles, but underestimates the amount of fine particles.

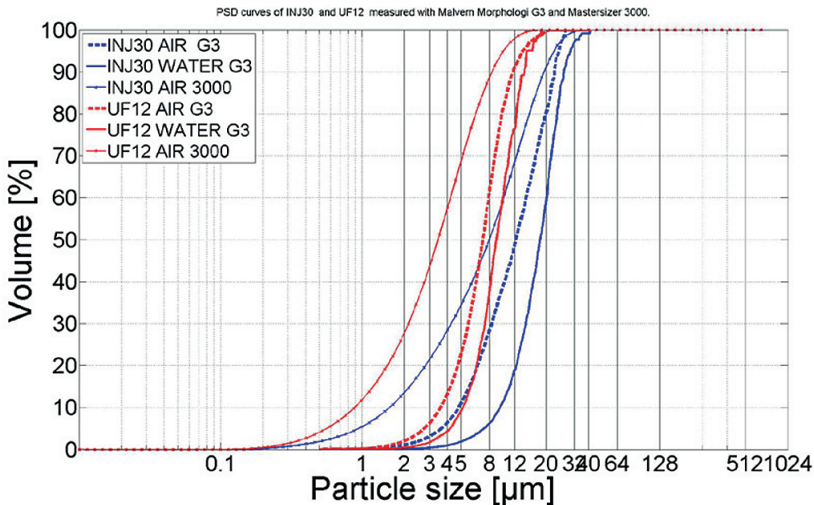


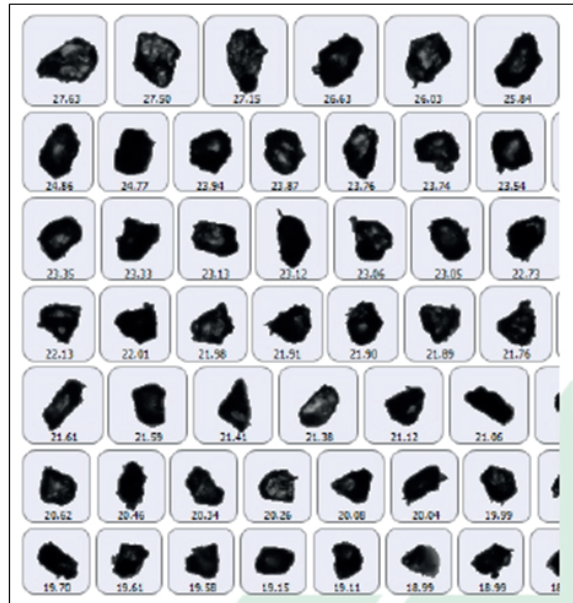
Figure 18: PSD curves of cements measured in Air (dry cement) and suspended in water measured with the Malvern Morphologi G3 and the Mastersizer 3000

Table 3: Characteristic particle diameter of 10%, 50% and 90% volume from measurements shown in Figure 18

| Characteristic particle diameter | UF12 | | INJ30 | |
|-----------------------------------|-------|------------------|-------|------------|
| | Dry | Water suspension | Dry | Suspension |
| D ₁₀ [μm] | 3.59 | 5.18 | 4.82 | 9.50 |
| D ₅₀ [μm] | 7.17 | 8.95 | 12.26 | 18.21 |
| D ₉₀ [μm] | 11.71 | 14.09 | 22.99 | 26.83 |



Cement suspended in water



Dry cement

Figure 19: Pictures of the largest particles of INJ30 cement measured with the Morphologi G3, from measurements presented in Figure 18

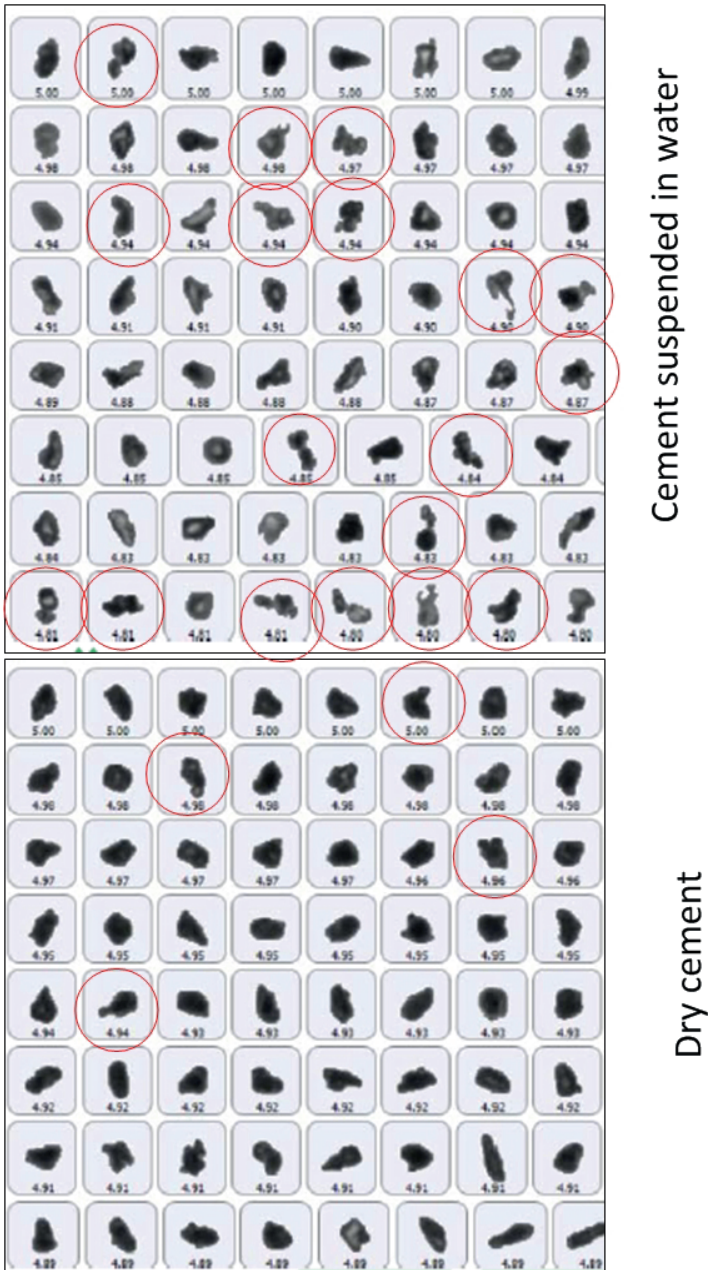
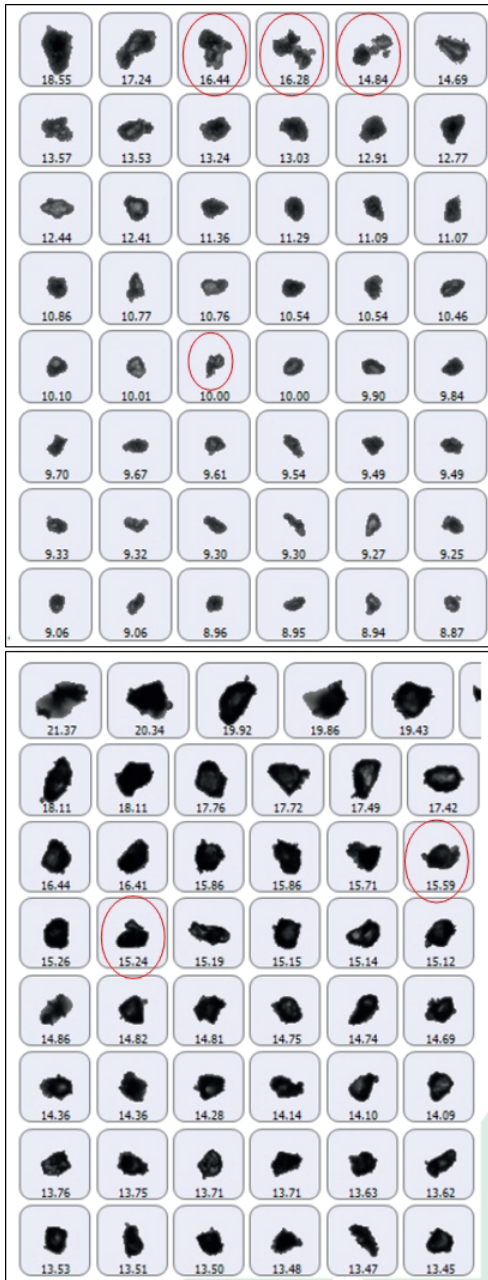


Figure 20: Pictures of the particles around 5 μm of INJ30 cement measured with the Morphologi G3, from measurements presented in Figure 18



Cement suspended in water

Dry cement

Figure 21: Pictures of the largest particles of UF12 cement measured with the Morphologi G3, from measurements presented in Figure 18

3.3.4. Summarized measurements of PSD curves with the presented methods

Sections 3.3.1 - 3.3.3 presented the PSD curves of INJ30 and UF12 estimated with different instruments in different media. From these measurements it can be concluded that PSD curves estimated with the Malvern Mastersizer 3000 in air give the most reliable results. Measurements with the Malvern Mastersizer S and the Malvern Mastersizer 3000 in alcohol show some smaller amounts of fine particles compared to measurements in air, which means that some fine particles in cement have flocculated with other particles.

Measurements in water showed that cement has a high tendency to flocculate and the dispersion process is important. The Morphologi G3 is suitable for studying the presence of oversized particles but underestimates the amount of fine particles. The measurements with this instrument showed that oversized particles in the tested sample generally consisted of assemblages of smaller particles but more measurements are needed for a better statistical representation of cement.

3.5. Penetration test, choice of grout recipe, and mixing method

Twenty penetration tests were performed with grouts based on INJ30 and UF12; eleven with a 70 μm slot, five with a 50 μm slot, and four with a 30 μm slot. Table 4 shows the grout recipes, mixing times, and the number of the tests performed with each slot. The PSD curves of the cements are shown in Figure 14.

Table 4: List of the penetration tests performed with grouts based on INJ30 and UF12 with 70, 50 and 30 μm slot

| Grout | 70 μm slot | | 50 μm slot | | 30 μm slot | |
|--------------------------|-----------------------|-----------------|-----------------------|-----------------|-----------------------|-----------------|
| | Mixing time | Number of tests | Mixing time | Number of tests | Mixing time | Number of tests |
| IN30,w/c=0.8,0.5%add | 10 min | 3 | 4 min | 3 | 4 min | 3 |
| UF12,w/c=1.0,0.5%add | 10 min | 3 | 4 min | 2 | 4 min | 1 |
| UF12,w/c=1.0,0.5%add | 4 min | 3 | - | - | - | - |
| UF12,w/c=1.0,whitout add | 4 min | 2 | - | - | - | - |

The grout recipes, i.e. w/c ratio and amount of admixture, were chosen on the basis of often used grouts in the field. The choice of grout mixing in the laboratory is difficult in the sense that the mixing should correspond to mixing in the field. The grouts are mixed with laboratory Dispermat CV3 dissolver with a rotor-stator system of 10,000 rpm, shown in Figure 22. Some penetration tests were performed too choose a proper mixing technique such as a rotor-stator system or disc and the proper rpm for the respective technique. During mixing, the whole amount of grout must be in motion to achieve proper mixing. When grout is mixed with a disc, a "donuts effect" is achieved when all amount of grout is in motion. See the illustration in Figure 22. This effect was achieved at 1,030 rpm. When mixing with a rotor-stator, a "boiling effect" occurs when the whole amount of grout is in motion. This effect was achieved at 6,450 rpm. The grout tested was UF12 w/c=1.2 and 0.5% iFlow. The results of the penetration test, presented in Figure 22, showed that the disc technique might be somewhat better. However, a rotor-stator system and 10,000 rpm were chosen because the producers of the cement and admixture use this type of mixing during their own product testing. According to their experience, the rotor-stator technique is better. This made it easier to compare these results with theirs.

Grout is mixed in a dispersion container with an inside diameter of 24 cm and 10 l capacity. The

distance between the rotor-stator axis and the bottom of the dispersion container was 25 mm. The grout batches are based on 3 l water. Mixing time was 10 or 4 minutes. The dispersion additive was added after one minute of mixing. The dispersion additive used is iFlow from Sika. According to the supplier, this dispersion additive has both a steric and an electrostatic repulsive force.

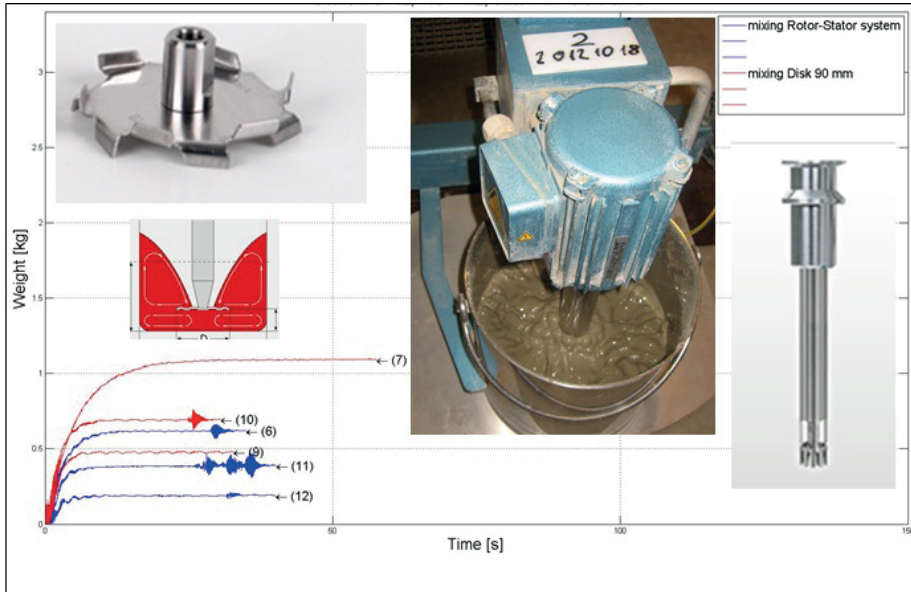


Figure 22: Penetration tests mixed with disc ($rpm=1,030$) and rotor-stator system ($rpm=6,450$). Grout tested UF12, $w/c=1.2$, 0.5% iFlow. $50 \mu\text{m}$ slot.

3.6. Results of penetrability measurements of UF12 and INJ30 based grouts

The results of penetration measurements of grouts based on INJ30 and UF12 cements tested with 70, 50, and $30 \mu\text{m}$ slots are presented in Figure 23. In the tests with all slots, the grouts based on INJ30 showed a much better penetrability than grouts based on UF12. These measurements showed that grouts based on INJ30 have a b_{critical} between 40 and $56 \mu\text{m}$ while grouts based on UF12 have a b_{critical} larger than $70 \mu\text{m}$.

In tests with a $70 \mu\text{m}$ slot, grouts based on INJ30 passed the slot in 13 s without any filtration in all three tests although the one side in this slot is $56 \mu\text{m}$.

In tests with grouts based on UF12 where mixing time was 10 minutes, the whole amount of grout passed the slot in one test. In the other two tests, a significant amount of grout also passed the slot. The average amount of grout passed in the three tests was 85%. In all three tests with UF12, regardless of all grout being passed or not, the grout was filtered. In two of three tests with UF12 with mixing time 4 minutes, the whole amount of grout passed the slot. In the third test, 61% of the grout passed the slot. The average penetration in these three tests was 87%, which is approximately the same penetrability as in previous tests.

In two tests with UF12 without admixture (without add), approximately half of the grout passed

the slot. The average penetrability in these two tests was 47%, which is lower than in tests with admixture. This shows that dispersion admixture has a significant effect on penetrability but penetrability is still lower than in grout based on INJ30.

Grouts based on INJ30 cement also showed better penetrability in the test with the 50 μm slot. The average penetration of grout based on INJ30 cement was 89%, while in grout based on UF12 the corresponding penetration was 32%, which is significantly lower.

The initial weight of grout in the grouting container should be around 4.430 kg for grouts with $w/c = 0.8$ (INJ30) and 4.183 kg for grout with $w/c = 1$ (UF12). The cement density used for calculation is 3.150 kg/m^3 . During testing, it was observed that the initial weight of the tested grouts was somewhat lower. The initial weights of grout tests in Figure 23 are shown in Table 5, Table 6, and Table 7. The reason for this variation is a large amount of air entrapped in the grout during the mixing. It can be seen that the amount of air in a grout is dependent on mixing time, the presence of admixture, and the cement's fines. Grouts based on INJ30, which is coarser cement than UF12, contain a significantly smaller amount of air despite the presence of admixture. Grout based on UF12 without admixture also contains significantly less air than corresponding grouts with admixture.

XRD analysis showed that UF12 has a somewhat higher amount of ettringite in hydrated cement. SEM analysis of filter cake from these grouts are performed to see if the reason for lower penetrability of UF12 could be ettringite, i.e. C_3A in cement or the presence of oversized particles, although measurements of PSD curves do not show any significant presence of oversized particles.

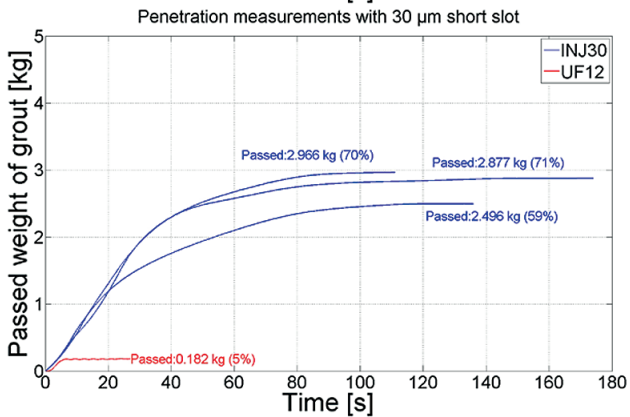
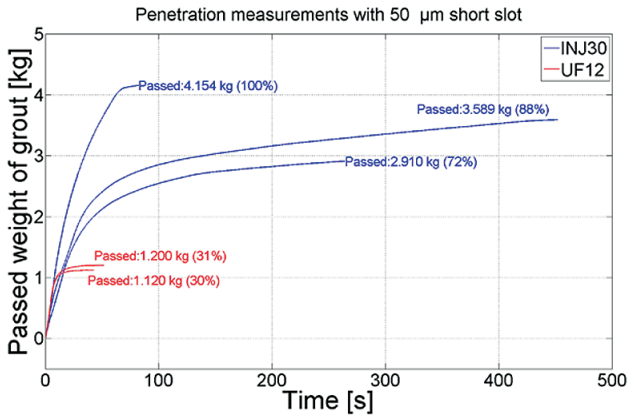
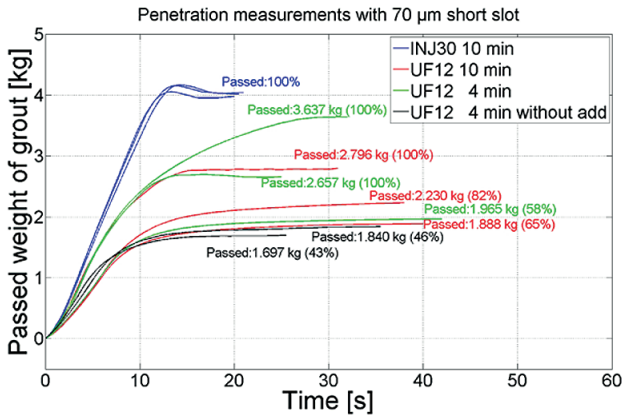


Figure 23: Penetration measurements with grouts based on INJ30 and UF12 with 70, 50 and 30 μm slots.

Table 5: The initial weight of grout in the grouting container in the test with 10 minutes of mixing

| | | | |
|----------------|-------|-------|-------|
| INJ30 w/c =0.8 | 4.219 | 4.250 | 4.113 |
| UF12 w/c=1 | 2.779 | 3.021 | 3.008 |

Table 6: The initial weight of grout in the grouting container in the test with 4 minutes of mixing.

| | | | | | | |
|----------------|-------|-------|-------|-------|-------|-------|
| INJ30 w/c =0.8 | 4.439 | 4.309 | 4.466 | 4.350 | 4.266 | 4.352 |
| UF12 w/c=1 | 2,800 | 3.897 | 3.506 | 3.829 | 3.902 | 3.831 |

Table 7: The initial weight of grout in the grouting container in the test without admixture

| | | |
|------------|-------|-------|
| UF12 w/c=1 | 4,151 | 4,125 |
|------------|-------|-------|

3.7. SEM analysis of filter cake of UF12 and INJ30 grout

The aim of the SEM analysis was to investigate the presence of oversized particles in cements, presence of needle-shaped gypsum crystals if possible and any agglomeration of cement particles caused by ettringite formation and fast hydration of C₃A.

Figure 24 shows two images of filter cake from INJ30 and UF12 grouts magnified 966 and 1028 times respectively. One important observation from these images is the presence of “fine” and “coarse” particles in filter cake in INJ30 and UF12 grouts. The image of INJ30 shows that most of the INJ30 consists of particles between 10 and 20 or 25 μm. According to PSD curve measurements, approximately 50% of INJ30 consists of these particles. According to this image, these particles make up a larger part of INJ30 than 50%. There is also a relatively large number of fine particles i.e. particles smaller than 3 or 4 μm. According to the PSD curve measurements, approximately 20 to 25% of INJ30 consists of these particles. Looking at the picture of filter cake from INJ30, it can be seen that these small particles are spread evenly in the filter cake and on the surfaces of larger particles. See the larger particle marked with a circle. The agglomeration of 5 to 10 small particles under 3 μm with this large particle in the range of 25 μm does not change the penetrability of this grout significantly. These small particles do not significantly influence the agglomeration of this large particle with other large particles around it as illustrated in Figure 1. The shearing between this particle and surrounding particles should be easy during flowing.

On the other hand, smaller particles around “medium size” particles might significantly influence agglomeration of these particles with surrounding particles. See the part of the image marked with a rectangle. Three or four “medium-sized” particles are surrounded by fine particles and an agglomerate is produced. It might be more difficult to shear this agglomerate at a constriction during flowing than those made up of larger particles. This might mean that reductions of both fine and medium-sized particles might improve penetration.

The lower picture in Figure 24 shows an image of a UF12 filter cake. The largest particles are in the range of 10 μm but most of the mass consists of “fine” and “medium-sized” particles. According to Figure 16, 35% are particles smaller than 3 μm (“fine”) and 45% particles between 3 and 8 μm “medium-sized”. This might mean that the grout which consists of these particles is much more difficult to disperse during mixing and to keep dispersed during the grouting or penetration measurements as showed with PSD measurements in water.

Figure 27 shows one oversized particle observed in INJ30 but this analysis is based on examination of two samples from INJ30 and two from UF12 cakes, which cover a very small area of the total filter cake.

Figure 28 shows a SEM image of UF12 magnified 16,815 times, where the bar in the image is 5 μm . The hydration process is stopped after 30 minutes by drying the sample in vacuum before measuring. The larger particles in the figure are connected to smaller particles even after drying. The smaller particles are not just lying on the larger particles; they are glued between and to larger particles. Otherwise, the whole filter cake structure would collapse. The larger the amount of fine particles the stronger the structure that needs to be sheared at constrictions.

An unusual assemblage of fine particles was observed in the UF12 filter cake. See the marked area in image a) in Figure 29. It is difficult to see if this is a large assemblage of fine particles or one large particle covered with small particles.

Figure 25 and Figure 26 show a filter cake of INJ30 and UF12 grouts with 3 and 4 times greater magnification than the images in Figure 24. An absence of small particles in INJ30 grout compared to the UF12 grout can also be observed. These pictures confirm measurements of PSD curves which show that INJ30 contains a lower amount of fine particles. This might be the most important difference between INJ30 and UF12 as regards penetrability since the SEM analysis did not show any significant presence of oversized particles in INJ30 or UF12 or needle formed ettringite.

More images of the INJ30 filter cake can be found in Appendix 3. Images from 2.2 mm x 2.2 mm to 40 μm x 40 μm are shown. It can also be seen that larger amounts of smaller particles between larger particles give larger and stronger assemblages.

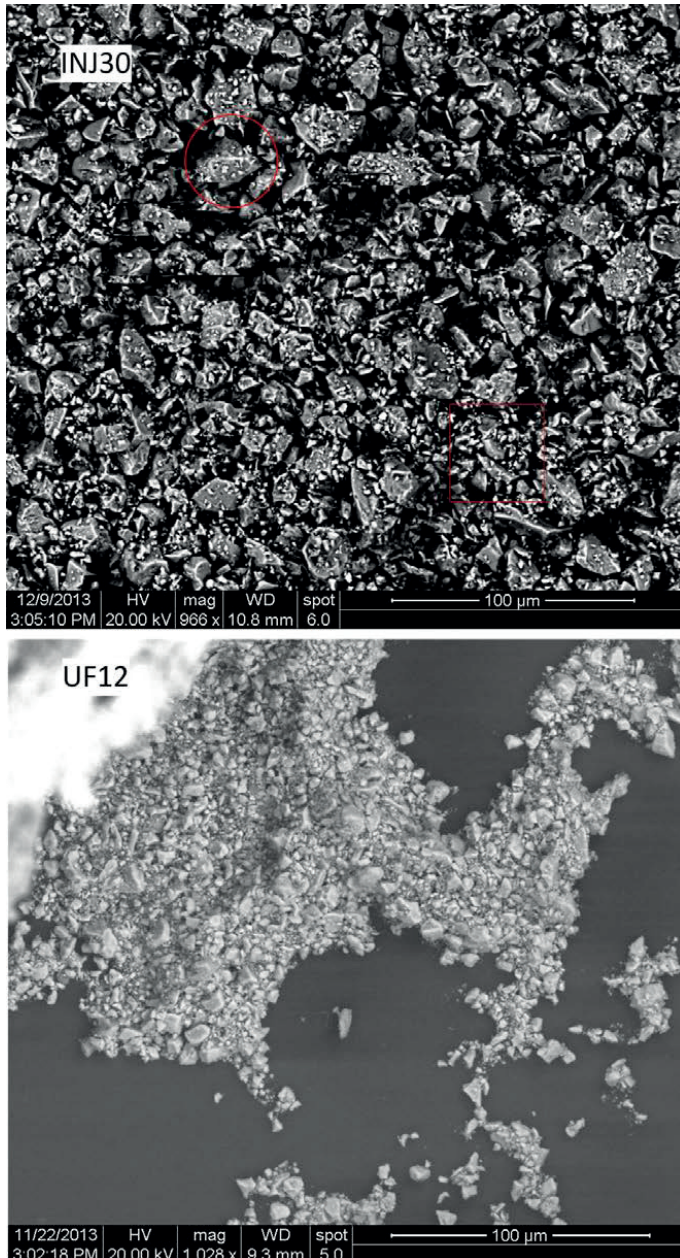


Figure 24: SEM images of filter cakes from INJ30 and UF12 grouts. Bar 100 µm.

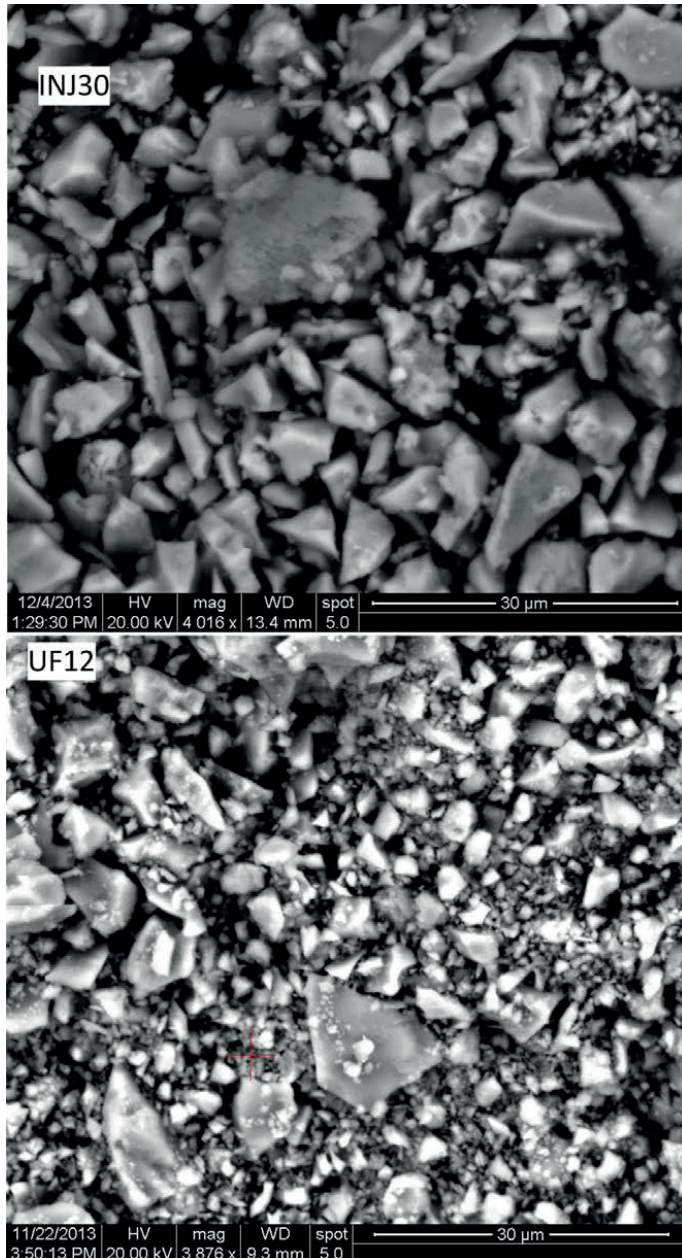


Figure 25: SEM images of filter cake from INJ30 and UF12 grouts. Bar 30 µm

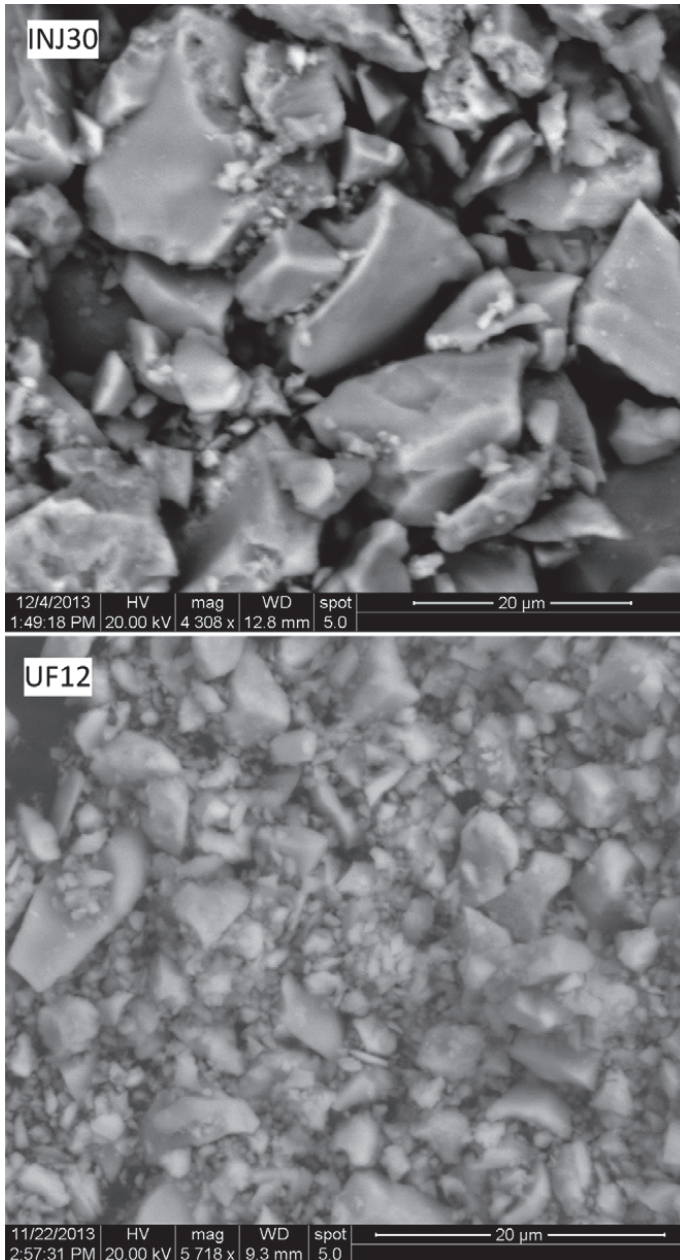


Figure 26: SEM images of filter cakes from INJ30 and UF12 grouts. Bar 20 µm.

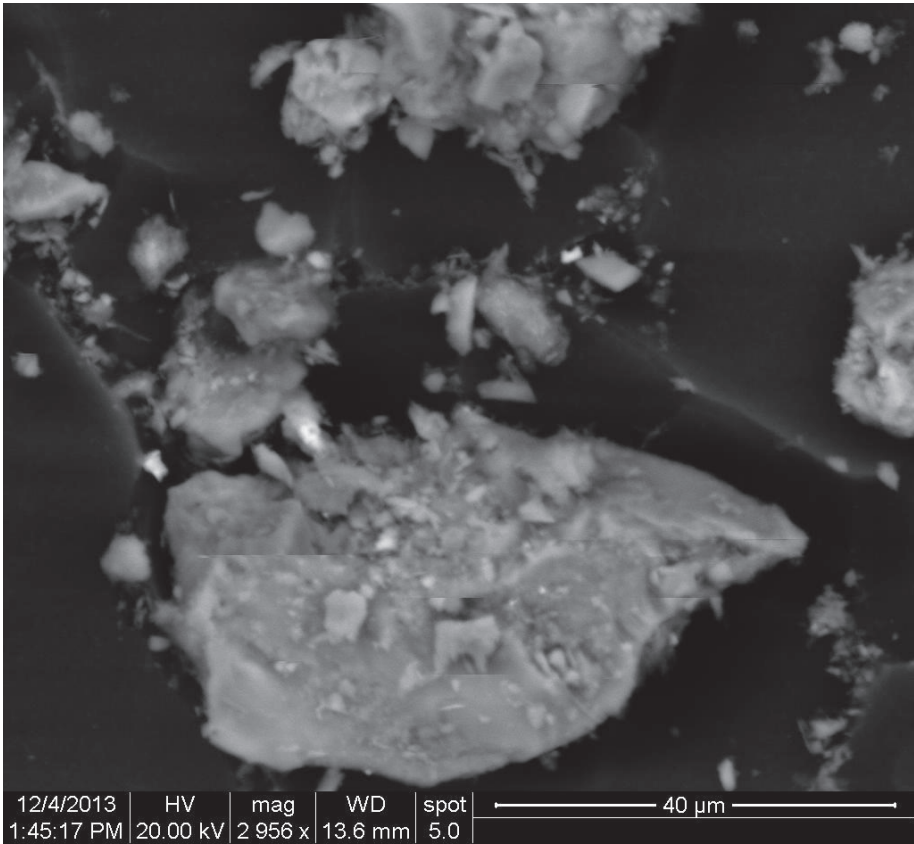


Figure 27: A large particle in INJ30 approximately 65 μm in length and 34 μm in width.

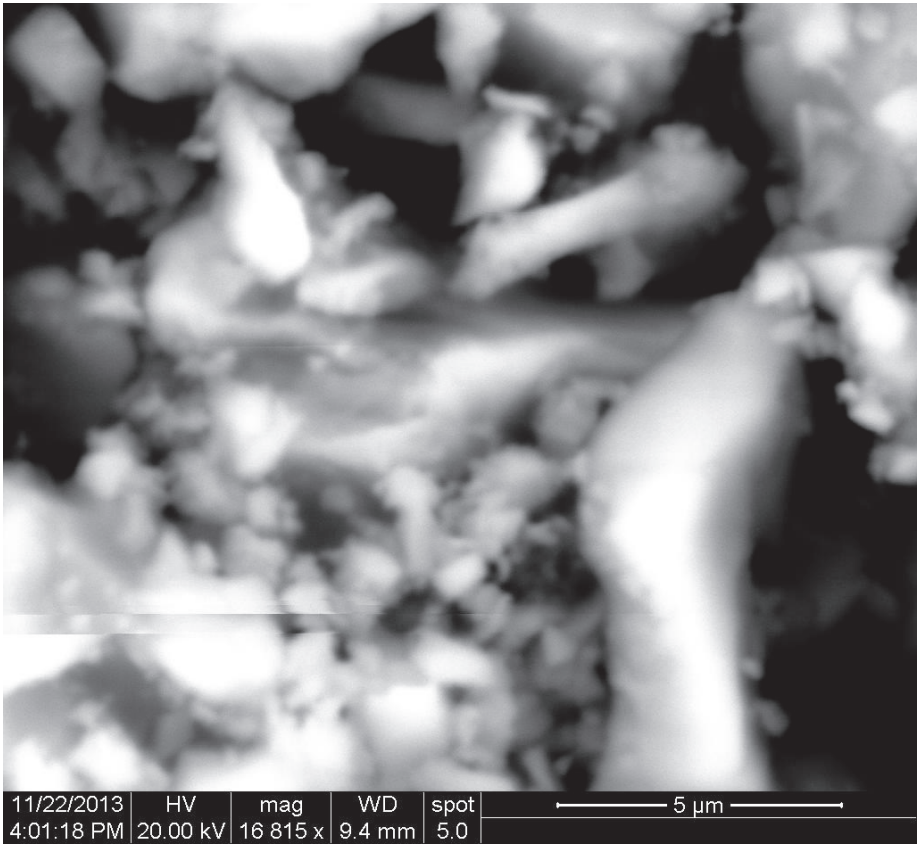


Figure 28: SEM image of a filter cake from a UF12 grout. Bar 5 μm. Magnification 16815.

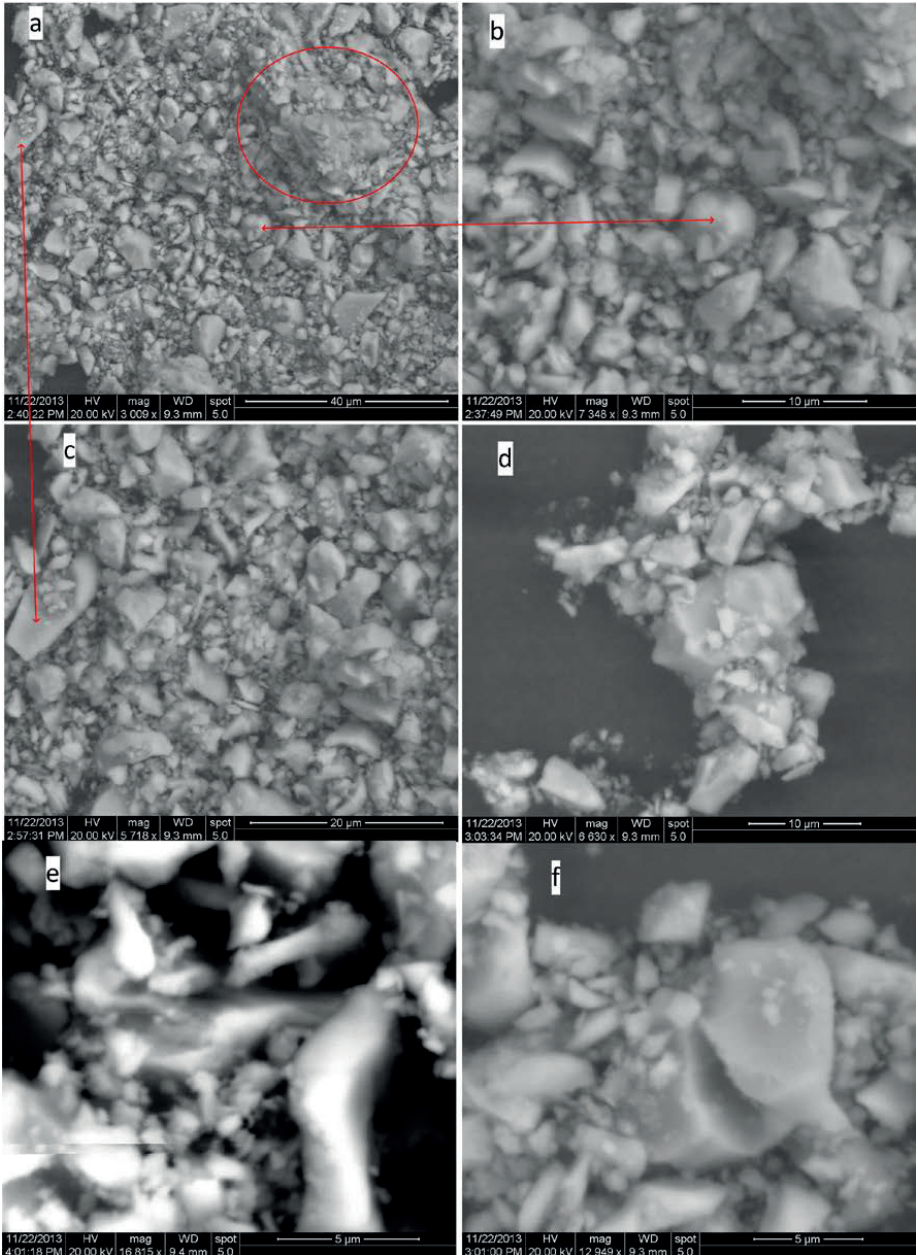


Figure 29: An unusual assemblage (image a) in a UF12 filer cake.

Image analysis with the SEM microscope did not show any presence of needle-shaped gypsum or ettringite crystals in filter cakes of INJ30 or UF12 cement pastes. No images similar to that shown in Figure 4, which was taken by ESEM, have been observed. They should be observable

even with SEM and in dried samples if they exist and are of similar size. They will probably be broken but still observable.

Chemical analysis of filter cakes with SEM did not show any particular differences between the INJ30 and UF12 filter cakes.

Column 1 in Table 8 shows an analysis of the INJ30 filter cake. The entire image area of the image shown in Figure 24 was analyzed. The size of the area is 270 μm by 270 μm . It shows a typical result of standard Anl aggningcement. When measurement is performed on a smaller area or a spot, some differences might occur between weight percent of oxides.

Table 8 also shows the results from three spot measurements of UF12 filter cake. The measuring points are shown in Figure 30. The aim of the measurement at points 1 and 2 was to analyze the content of smallest particles. At point 2, the amount of aluminum and iron oxides was larger than average. It could be a place where content of C₃A and C₄F is somewhat larger than average. In this investigation, no special particles were observed. See point 3 in the lower images in Figure 30. The particle is formed as a perfect ball with a small pyramid glued to it. Chemical analysis showed that this particle consisted mostly of silicon and aluminum dioxide.

Table 8: SEM chemical analysis of filter cake of INJ30 and UF12 grouts. Weight [%].

| | INJ30 Analysis of whole area of image presented in Figure 24 [270 μm x 270 μm] | INJ30 Analysis of an area of 15 μm x 15 μm . | UF12 Point 1 Figure 30 | UF12 Point 2 Figure 30 | UF12 Point 3 Figure 30 |
|--------------------------------|---|--|------------------------------|------------------------------|------------------------------|
| Oxides | Weight [%] | Weight [%] | Weight [%] | Weight [%] | Weight [%] |
| CaO | 64.19 | 57.54 | 72.21 | 56.11 | 13.30 |
| SiO ₂ | 21.11 | 22.69 | 15.85 | 23.73 | 49.99 \uparrow |
| Al ₂ O ₃ | 5.37 | 6.82 | 3.49 | 7.70 | 24.84 \uparrow |
| Fe ₂ O ₃ | 4.64 | 7.71 | 5.05 | 4.96 | 9.97 |
| SO ₃ | 1.99 | 2.04 | 2.64 | 5.01 | - |
| MgO | 1.94 | 1.77 | - | 2.49 | - |
| Na ₂ O | 0.38 | 0.38 | - | - | - |
| K ₂ O | 0.38 | 0.46 | 0.76 | - | 1.89 |
| TiO ₂ | - | 0.59 | - | - | - |
| Total | 100.00 | 100.00 | 100 | 100 | 100.00 |

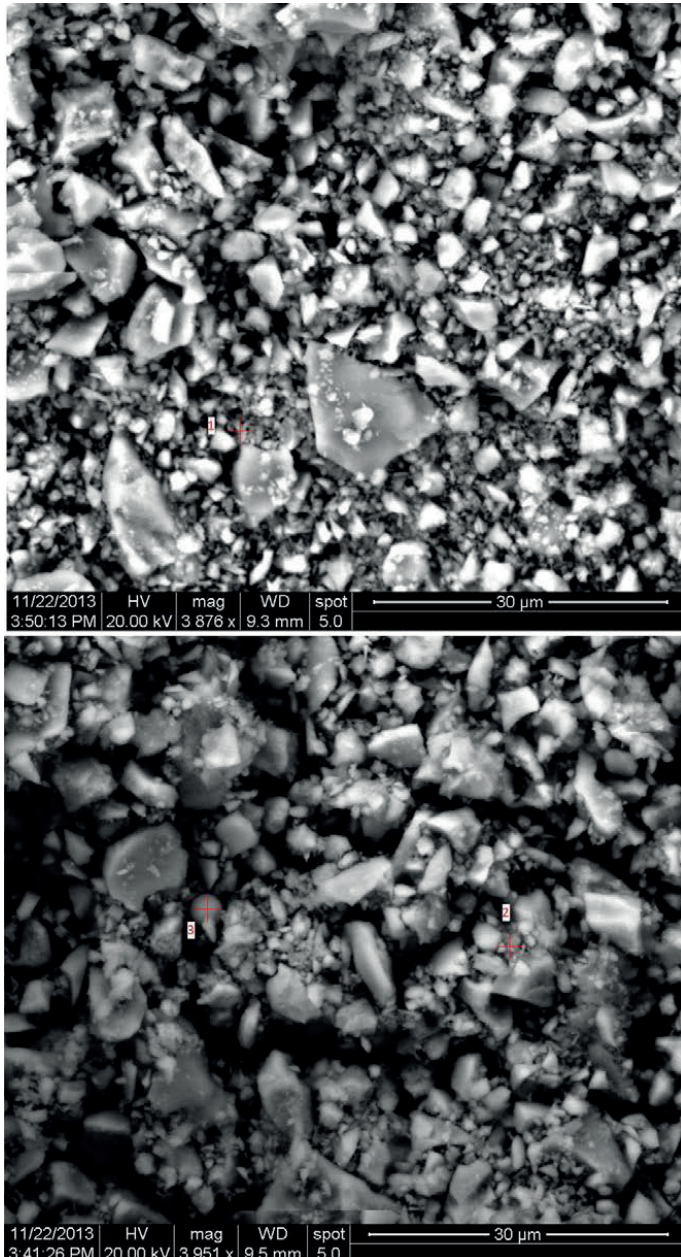


Figure 30: SEM image of UF12 filter cake. Three points where chemical spot analysis was performed.

3.8. Discussion of measurements with INJ30 and UF12

Penetration measurement with INJ30 and UF12 in this study confirmed previous research findings that grouts based on cement with a d_{95} of $30\ \mu\text{m}$ have better penetrability than grouts based on finer-ground cement with a d_{95} of $12\ \mu\text{m}$. (Eklund and Stille, 2008; Draganović and Stille, 2011; Pantazopoulos et al. , 2012).

XRD analysis showed that UF12 and Modified UF12 had a somewhat lower content of gypsum than INJ30. The part of gypsum in UF12 and Modified UF12 has converted to hemihydrates during grinding due to the high grinding temperature. Hemihydrates are more soluble in water and contact with water may cause secondary gypsum formation. This might also contribute to lower penetrability of UF12 but this was not observed in SEM analysis of filter cakes. SEM measurements showed that oversized particles are probably not the main problem even if they occur in the cement. A relatively small amount of cement was tested to exclude total this uncertainty. A larger amount of cement should be tested to obtain a more reliable result.

The PSD curves of the examined cements were measured with different instruments and in different media. Measurements with the Mastersizer 3000 in air are generally reliable. Measurements with the Mastersizer S and Mastersizer 3000 in alcohol underestimate the amount of fine particles smaller than $1\ \mu\text{m}$ by about 5% and might also overestimate the size of the largest particles, in particular in UF12.

SEM and PSD curve analysis in air, alcohol, and water shows that cement is sensitive to flocculation. It is probably easier to disperse agglomerations consisting of larger particles (10 to $20\ \mu\text{m}$) and small particles flocculated on their surfaces than agglomerates consisting of “medium-sized” particles, i.e. particles of between 3 and $8\ \mu\text{m}$ and small particles. This also means that it will be harder to shear flocks consisting of medium-sized and small particles than flocks consisting of larger and smaller particles when the grout has to pass a constriction. If the amount of small particles in grouts is large and can cover all medium-sized and large particles, it will be difficult to shear the flocks.

4. Measurements with T-cements

4.1. Introduction

The goal of testing with T-cements was to investigate if reduction of fine particles alone can improve penetrability. T-cements are therefore produced from a mix of INJ30 and UF12 and should have the same chemical content as INJ30 and UF12. If penetrability of the grout is related to the PSD curve of the cement, i.e. the amount of fine particles in cement, then grouts based on T-cement should show a better penetrability than UF12 based grouts. If the hemihydrates in UF12 contribute to lower penetrability, penetrability cannot be improved merely by reducing the amount of fine particles in T-cement.

4.2. Manufacturing of T cements

The cement is produced and supplied by Nauplion AB. T-cements are produced from a mix of INJ30 and UF12 with further sieving and milling. The cement particles are crushed by a punch with a rotating propeller inside the mill housing. One important difference compared to grinding process used during production of INJ30 and UF12 (Figure 13) is heating of the cement during grinding. The cements are not heated significantly during the grinding but base cements INJ30 and UF12 are already heated in their production.

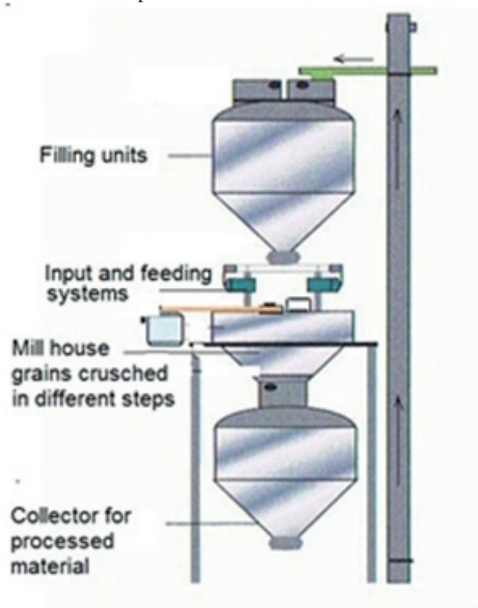


Figure 31: Illustration of manufacturing process for T and SP-cements

4.3. Measured PSD curves of specially produced T-cements

To study how the amount of fine particles influences the penetrability of grout, a number of T-cements were specially produced. The aim during production was to minimize the amount of particles smaller than $4\ \mu\text{m}$ as much as possible but with a process which could still be economically viable. The PSD curves of produced and tested T-cements are shown in Figure

32. The measurements are performed in alcohol using the Malvern Mastersizer S. Only the PSD curves of T13 were measured with the Mastersizer 3000 in air. Measurements in air are more reliable according to the measurements presented in paragraph 3.3.2. Measurements in alcohol show somewhat lower amounts of fine particles in cement compared to measurements in air and mostly those smaller than $1\mu\text{m}$ up to 5-10%. Table 9 shows the reduced amount of fine particles in T-cements compared to UF12. The amount of particles smaller than $4\mu\text{m}$ is between 25% and 42% and is reduced to between 5% and 33% for most of the cements. The highest reduction is achieved in the T12 cement. The amount of fine particles smaller than $4\mu\text{m}$ is reduced from 33% to 14% of the volume. The reduction in fine particles is smallest in T13 cement. It is important to note that reduction in this cement is compared with the other curve for UF12, also measured in air. With the exception of T12, the amount of fine particles in these cements is still higher than in INJ30.

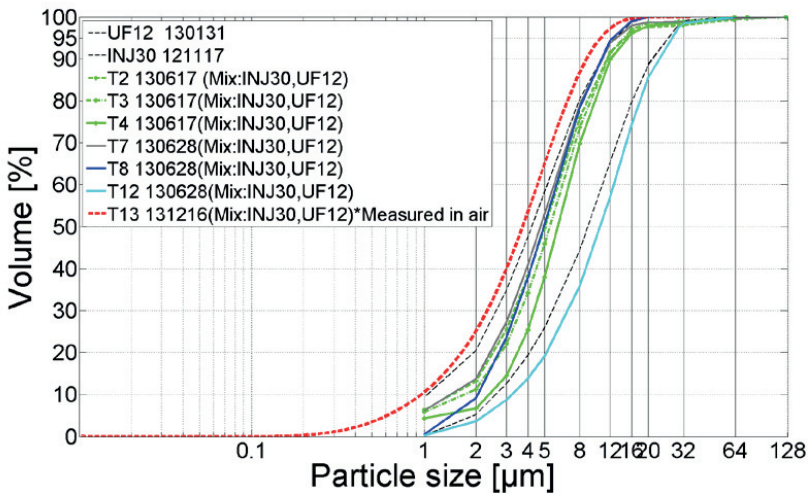


Figure 32: PSD curves of T-cements related to UF12 and INJ30 and measured with the Mastersize S in alcohol. T13 is measured with the Mastersize 3000 in air.

Table 9: Reduced amounts of fine particles in volume [%] compared to UF12 measured in alcohol.

| | T2,T3,T7,T8 | T4 | T12 | T13* |
|------------------|-------------|----|-----|------|
| < $1\mu\text{m}$ | 5 | 5 | 10 | 2* |
| < $2\mu\text{m}$ | 8 | 12 | 15 | 3* |
| < $4\mu\text{m}$ | 12 | 22 | 33 | 5* |

* PSD curves of T13 are measured in air and compared with UF12 also measured in air. Measurements in alcohol underestimate the amount of fine particles.

Figure 33 shows the largest particles of T-cement presented in Figure 32. The maximum particle size should be around $20\mu\text{m}$. It can be seen that T13 has no oversized particles, i.e. particles larger than $30\mu\text{m}$. T8 cement does not contain oversized particles either, despite the PSD curves being measured in alcohol. Other T-cements contain oversized particles up to $128\mu\text{m}$. The question is if these particles are agglomerates or individual particles. Since they are produced from a mix of UF12 and INJ30, they are probably the result of agglomeration.

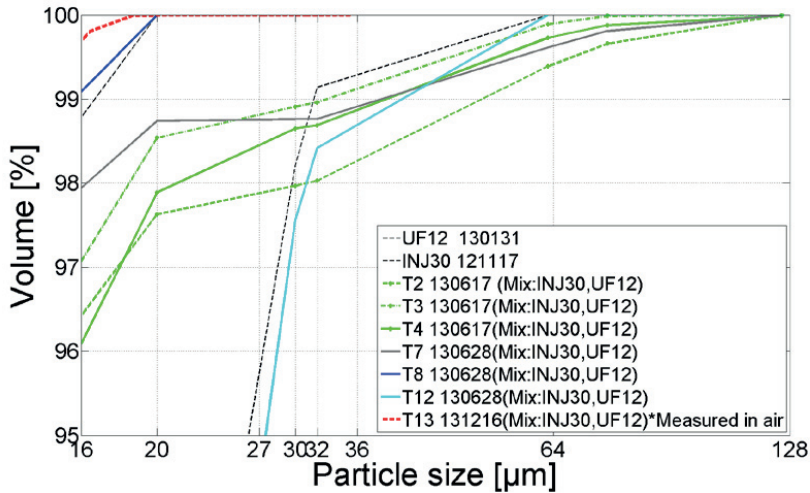


Figure 33: Enlarged PSD curves of larger particles of the T-cements shown in Figure 32.

4.4. Performed penetrability measurements with T-cements

Eight penetration measurements with the 50 µm slot were performed with grouts based on specially produced T-cements. Mixing time and recipe are the same as in the tests with UF12 with the 50 µm slot, i.e. w/c= 1.0 and additive 0.5% of cement weight.

4.5. Results of penetrability measurements of grouts based on T-cement

In specially produced T-cements, the amount of fine particles is reduced compared to UF12. This reduction should improve the penetrability of these grouts due to less flocculation. The results from penetration measurements of grouts based on these cements are shown in Figure 34.

T2, T3, T4, T7, and T8 showed a very low penetrability. In principle, a direct stop occurred in all six measurements. Quantities of particles smaller than 2µm are reduced from 20% to a range from 14% to 7% compared to UF12. Quantities of particles smaller than 4µm are reduced from 48% to between 42% and 25%. These cements showed a large amount of oversized particles. The oversized particles are probably a result of flocculation since base cements UF12 and INJ30 do not contain significant amounts of oversized particles.

T13 and T12 showed a better penetrability than other T-cements. T12 and T13 both have a lower amount of fine particles and a lower amount of oversized particles than other T-cements or UF12. This could be the reason why they showed better penetrability than other T-cements.

T13 and T12 showed penetrability in the same range as UF12 despite fewer fine particles. Since T-cements are produced partially from UF12, some chemical component in UF12 might be the reason why they did not show a better penetrability than UF12.

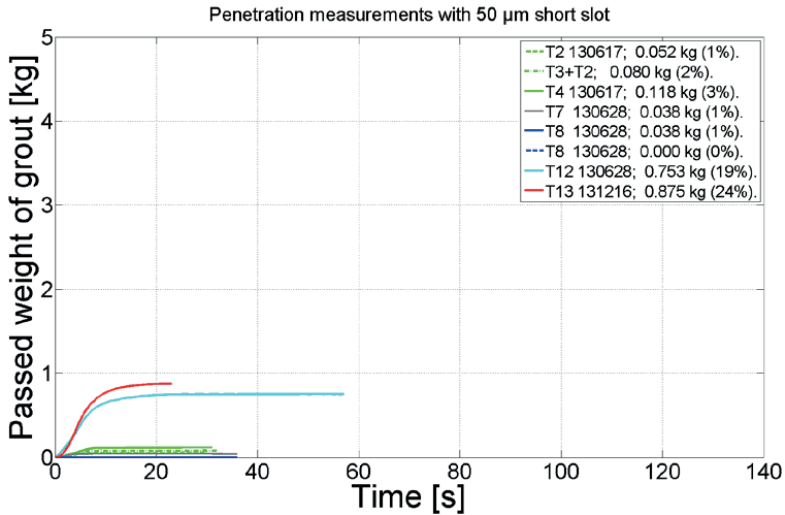


Figure 34: Penetration measurements with grouts based on specially produced T cement with 50 µm slots

4.6. Discussion of measurements with T-cements

In specially produced T12 and T13 cements, the amount of fine particles has been reduced significantly compared to UF12, but penetrability is in the same range as UF12, indicating that there is something else in these cements that they share with UF12 which deteriorates penetration. This might be some chemical component in UF12 such hemihydrates.

5. Measurements with SP-cements

5.1. Introduction

To study if there is some reason in UF12 other than large amounts of fine particles which deteriorate penetration of fine-milled cements, some preliminary penetration tests were performed with fine-milled cements based on other Portland cements and not on UF12 and INJ30. These are called SP-cements.

5.2. Manufacture of SP-cements

SP-cements are produced in the same machinery as T-cement by further grinding and sieving of other ordinary Portland cements. One important difference compared to the grinding process used during production of INJ30 and UF12 is heating of the cement during grinding. The SP-cements are not heated significantly during grinding and the risk of converting gypsum to hemihydrate is eliminated. The cement is produced and supplied by Nauplion AB.

5.3. Measured PSD curves of specially produced SP-cement

The PSD curves of SP-cements are shown in Figure 35. The measurements are performed in alcohol using the Malvern Mastersizer S. The PSD curves of SP4 and SP5 cements were measured with the Mastersizer 3000 in air.

The amount of particles smaller than $4\ \mu\text{m}$ is between 25% and 42% (Figure 35). The amount of fine particles compared to UF12 is reduced to between 5% and 20% (Table 10) for most of the cements. The reduction of particles smaller than $1\ \mu\text{m}$ is larger in SP-cements than in T-cements.

Figure 36 shows the largest particles of the SP-cement presented in Figure 35. The SP-cements also contained much lower amounts of oversized particles than T-cements.

Figure 37 shows the PSD curves of SP4 and SP5 cements compared to T13, UF12, and INJ30 all measured in air. It can be seen that the amount of fine particles ($<4\ \mu\text{m}$) is reduced by 15% in SP4 and SP5 compared to UF12 and T13, and the largest particles in SP4 and SP5 are $10\ \mu\text{m}$ smaller than in INJ30.

It is important to state that SP4 and SP5 have reduced amounts of fine particles, do not have oversized particles, and do not contain UF12. They should show a better penetrability.

Table 10: Reduced amounts of fine particles in volume [%] compared to UF12 measured in alcohol.

| | SP0 | SP1,SP2,SP3 | SP4*,SP5* |
|--------------------|-----|-------------|-----------|
| $< 1\ \mu\text{m}$ | 10 | 10 | 5* |
| $< 2\ \mu\text{m}$ | 11 | 13 | 10* |
| $< 4\ \mu\text{m}$ | 17 | 18-20 | 17* |

* PSD curves of SP4 and SP5 are measured in air and compared with UF12 also measured in air. Measurements in alcohol underestimate the amount of fine particles.

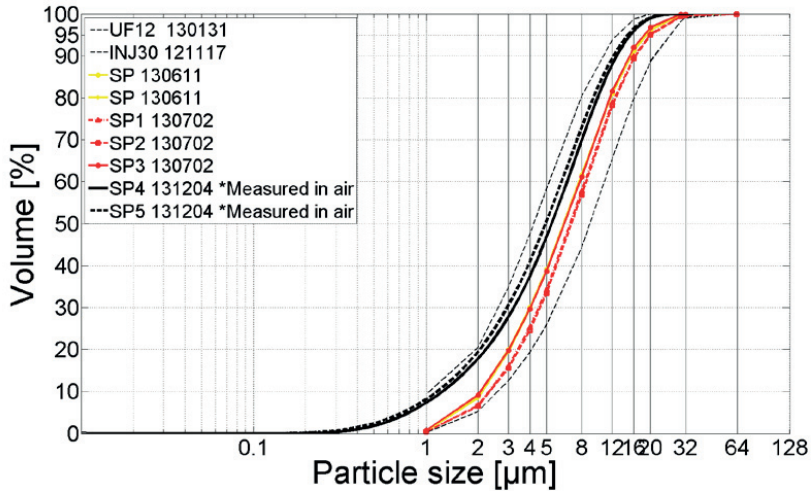


Figure 35: PSD curves of SP-cements related to UF12 and INJ30 and measured with the Mastersize S in alcohol. SP4 and SP5 are measured with the Mastersize 3000 in air.

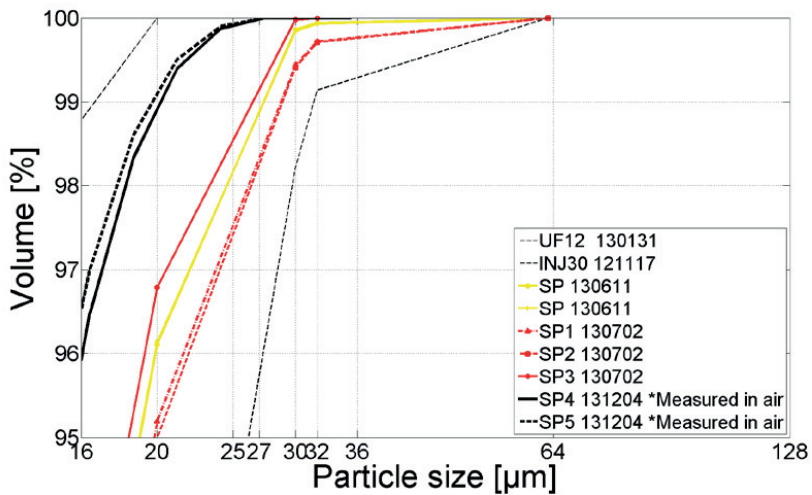


Figure 36: Enlarged PSD curves of larger particles of the SP-cement shown in Figure 35.

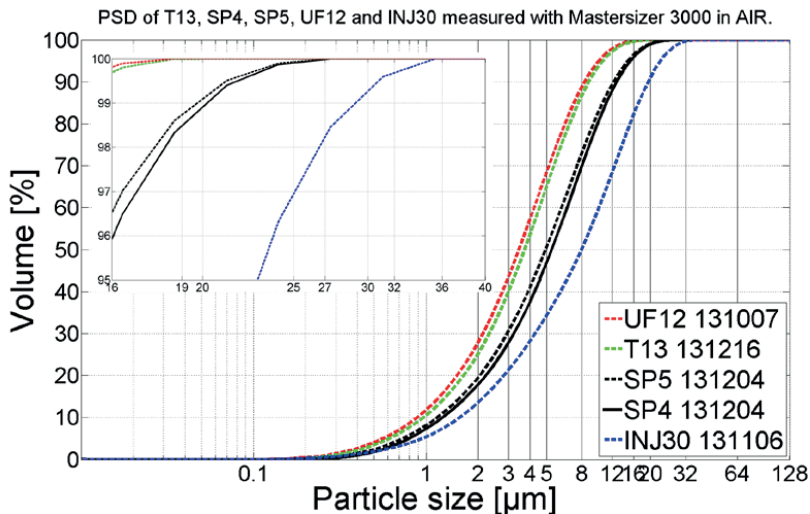


Figure 37: PSD curves of T13, SP4, SP5, UF12, and INJ30 measured with the Mastersizer 3000 in air.

5.4. Performed penetrability measurements with SP-cements

A further eight penetration measurements were performed with grouts based on SP-cements with the 50 µm slot. Mixing time and recipe are the same as in the tests with UF12 with the 50 µm slot, i.e. w/c= 1.0 and additive 0.5% of cement weight.

5.5. Results of penetrability measurements of grouts based on SP-cements

Figure 38 shows the results from penetrability measurements of grouts based on SP-cements. These cements showed a better penetrability than T-cements. The penetrability of SP 130611 cement was relative low and the penetrability of SP1 and SP2 grouts was in the same range as UF12 grouts. SP1 and SP2 contained particles of up to 64 µm. The reason might be flocculation or oversized particles. See Figure 36.

SP3 showed a better penetrability than UF12. The maximum particle size measured in SP3 cement was 30 µm. This test shows that it is important to minimize the amount of oversized particles in cement. However, even these grouts showed a lower penetration than INJ30-based grouts.

Grouts based on SP4 and SP5 cements showed the best penetrability and passed the 50 µm slot 100%. They showed the same penetrability as grouts based on INJ30 or even better. In one of three tests with INJ30, 100% of the grout passed and in the other two tests approximately 80% passed. It must be noted that both in SP4 and SP5 tests and in all tests with INJ30, the grouts were filtered during penetration.

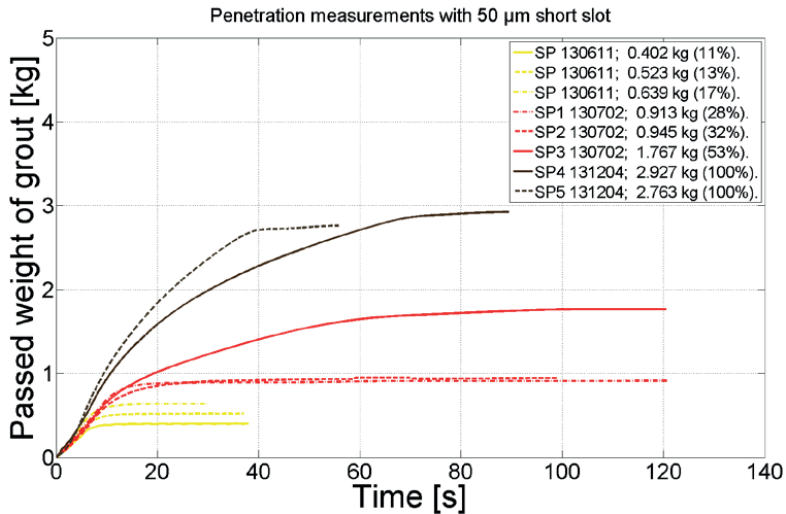


Figure 38: Penetration measurements with grouts based on specially produced SP-cement with 50 µm slots

5.6. Discussion of measurements with SP-cements

It is difficult to know why SP4 and SP5 are better than other SP-cements since detailed chemical content of SP-cements is unknown. SP4 and SP5-cements had approximately same amount of fine particles even if according to Figure 35 PSD-curve of SP4 and SP5-cements have larger amounts of fine particles than other SP-cements. SP4 and SP5 are measured in air and not in alcohol. Measurements in alcohol underestimate the amount of fine particles.

Comparing the PSD curves of SP4 and SP5 with T13 and UF12 and INJ30 (Figure 37), where the PSD curves were measured with the same method, it can be seen that the amount of fine particles was significantly reduced in SP4 and SP5. Since both the PSD curve and the base cement were changed, it is not clear which measure contributed to improved penetrability.

6. Discussion

Penetration measurement with INJ30 and UF12 in this study confirmed previous research findings that grouts based on cement with a d_{95} of $30\ \mu\text{m}$ have better penetrability than grouts based on finer-ground cement with a d_{95} of $12\ \mu\text{m}$. (Eklund and Stille, 2008; Draganović and Stille, 2011; Pantazopoulos et al., 2012).

XRD analysis showed that UF12 had a somewhat lower content of gypsum than INJ30. The part of gypsum in UF12 has probably converted to hemihydrates during grinding due to the high grinding temperature. More soluble hemihydrates in contact with water may cause secondary gypsum formation. This might also contribute to lower penetrability of UF12 but it was not observed in SEM analyses of filter cakes. SEM measurements showed that oversized particles are probably not the problem even if they occur in the cement. A relatively small amount of cement was tested to exclude this uncertainty.

T-cements are produced from a mix of INJ30 and UF12, where the amounts of fine particles are reduced to test if this reduction can improve penetrability. These cements did not show a better penetrability, which also indicate that there is something else in these cements that they have common with UF12 which deteriorate penetration. This might be some gypsum-related chemical component in UF12.

SP4 and SP5 cements showed much better penetrability than UF12 or T-cements. The penetrability was in the same range as INJ30 or better and they could be used to grout $50\ \mu\text{m}$ fractures or even smaller. These SP-cements also had lower amounts of fine particles than UF12 or T-cements. Property d_{100} of SP4 and SP5 cement was $27\ \mu\text{m}$ and the amount of fine particles ($< 1\ \mu\text{m}$, $< 2\ \mu\text{m}$, and $< 4\ \mu\text{m}$) was reduced by 5%, 10%, and 17% respectively compared to UF12. The largest particles in SP4 and SP5 are around $27\ \mu\text{m}$ and in INJ30 $35\ \mu\text{m}$. Since these SP-cements are produced from other Portland cement, it is not clear if reduced amounts of fine particles in cements or different base cements led to improved penetrability.

The PSD curves of the examined cements were measured with different instruments and in different media. Measurements with the Mastersizer 3000 in air are generally most reliable. Measurements with the Mastersizer S and Mastersizer 3000 in alcohol underestimate the amount of fine particles. Measurements with the Mastersizer 3000 in air should be used in all measurements in further research if possible. In this case, uncertainty in comparisons of PSD curves between different cements will be minimized. The measurements of the presence of oversized particles could also be performed with the Morphology G3.

SEM and PSD curve analysis in air, alcohol and water shows that cement is sensitive to flocculation. It is probably easier to disperse agglomerations consisting of larger particles (10 to $20\ \mu\text{m}$) and small particles flocculated on their surfaces than agglomerates consisting of “medium-sized” particles, i.e. particles of between 3 and $8\ \mu\text{m}$ and small particles. This also means that it will be harder to shear flocks consisting of medium-sized and small particles than flocks consisting of larger and smaller particles when the grout has to pass a constriction. If the amount of small particles in grouts is large and can cover all medium-sized and large particles, it will be difficult to shear the flocks.

In future investigation of gypsum's and ettringite's role in the penetrability of cement-based grouts, a better SEM technology such as ESEM-EDX should be used. Filter cake or initial grout should be investigated without evaporation of samples or pressing out pore water.

7. Conclusions

This study confirms previous research findings (Eklund and Stille, 2008; Draganović and Stille, 2011; Pantazopoulos et al. , 2012) that grouts based on ordinary Portland cement with a d_{95} of 30 μm have better penetrability than grouts based on more finely ground cement with a d_{95} of 12 μm .

Chemical analysis of INJ30 and UF12 and penetration tests with T- and SP-cements indicate that not just the amount of fine particles in cements is important for penetration but also the chemical content of cement such as content of gypsum and its form in cement as dihydrate or hemihydrate might be important.

Measurements of SP-cements showed that the penetrability of grouts based on fine-milled cement can be further improved. Since the detailed chemical content of tested SP-cements is not known, it is not clear what the main reason for the improved penetrability is.

In future research, both the amount of fine particles, d_{100} , and the chemical content of the cement must be considered. More different cements should be investigated. PSD curves should be measured in air. Measurements in alcohol underestimate the amount of fine particles, which tend to flocculated with larger ones. The presence of ettringite should be investigated in wet conditions in initial grout, preferably with an ESEM microscope to avoid drying and destruction of any ettringite crystals in the sample or perhaps flushing them from the grout during filtration.

8. References

- Betonghandbok, Material. (1994). Stockholm: Svensk Byggtjänst AB.
- Draganović, A., Stille, H., 2011. Filtration and penetrability of cement-based grout: Study performed with a short slot. *Tunnelling and Underground Space Technology* 26, 548–559.
- Eklund, D., Stille H., 2008. Penetrability due to filtration tendency of cement-based grouts. *Tunnelling and Underground Space Technology* 23, 389-398.
- Gandolfi, M.G., van Landuyt, K. Taddei, P. Modena, E. van Meerbeek, B Prati. C. 2010. Environmental Scanning Electron Microscopy Connected with Energy Dispersive X-ray Analysis and Raman Techniques to study ProRoot Mineral Trioxide Aggregate and Calcium Silicate Cements in wet Conditions and in Real Time. *Journal of Endodontics*, 36, 5, 851-857.
- Pantazopoulos, I.A., Markou, I.N., Christodoulou, D.N., Droudakis, A.I., Atmatzidis, D.K., Antiohos, S.K., Chaniotakis, E., 2012. Development of microfine cement grouts by pulverizing ordinary cements, *Cement and Concrete Composites*, 34, 5, 593-603.
- Ramachandran, V.S., Malhotra, V.M., Jolicoeur, C., Spiratos, N.. 1998. Superplasticizers: Properties and Applications in Concrete . Book. ISBN 0-660-17393-X.
- Scrivener, K.L., Fullmann, T., Galluccia, E., Walentab, G., Bermejo. E., 2004. Quantitative study of Portland cement hydration by X-ray diffraction/Rietveld analysis and independent methods. *Cement and Concrete Research* 34, 1541–1547
- Zingg, A., Holzer, L., Kaech, A., Winnefeld, F., Pakusch, J., Becker, S. Gauckler. L. 2008. The microstructure of dispersed and non-dispersed fresh cement pastes — New insight by cryo-microscopy. *Cement and Concrete Research* 38, 522–529.

Appendix 1: Anlæggingscement, Technical Data Sheet

Technical data

Anlæggingscement CEM I 42,5 N - SR 3 MH/LA

Anlæggingscement complies with the data below.

On rare occasions the values may deviate from the specified ranges or limits.

Physical data

| PROPERTY | GUIDELINE VALUE | RANGE | UNIT | REQUIREMENT | CURRENT STANDARD |
|---------------------------|-----------------|-------|--------------------|-----------------|------------------|
| Blaine fineness | 310 | ± 30 | m ² /kg | | |
| Setting time | 150 | + 30 | min | ≤ 60.0 | EN 197-1 |
| Compressive strength 1 d* | 10 | + 3 | MPa | | |
| Compressive strength 2 d* | 20 | + 3 | MPa | ≤ 10.0 | EN 197-1 |
| Compressive strength 7 d* | 35 | + 4 | MPa | | |
| Compressive str. 28 d* | 54 | + 4 | MPa | ≤ 52.5 & ≤ 62,5 | EN 197-1 |
| Heat of hydration 1 d | 170 | + 20 | kJ/kg | | |
| Heat of hydration 3 d | 240 | + 20 | kJ/kg | | |
| Heat of hydration 7 d | 270 | + 20 | kJ/kg | ≤ 290 | SS134202 |
| Compact density | 3200 | + 20 | kg/m ³ | | |
| Bulk density | 1250 | + 250 | kg/m ³ | | |
| Brightness | 21 | + 1 | % | | |

*Measured on standard mortar

Chemical data

| PROPERTY | LIMITS | UNIT | REQUIREMENT | CURRENT STANDARD |
|--|-----------|------|-------------|------------------|
| Loss on ignition | 0.5-1.5 | % | ≤ 5.0 | EN 197-1 |
| Insoluble residue | 0-0.2 | % | ≤ 5.0 | EN 197-1 |
| Magnesium oxide, MgO | 0.8-1.0 | % | ≤ 5.0 | EN 197-1 |
| Sulfates, SO ₃ | 2.3-2.5 | % | ≤ 3 | EN 197-1 |
| Chloride, Cl | 0.01-0.03 | % | ≤ 0.10 | EN 197-1 |
| Tricalcium aluminate, C ₃ A | 1.5-2.5 | % | ≤ 3 | EN 197-1 |
| Alkali, equiv. Na ₂ O | 0.40-0.55 | % | ≤ 0.6 | SS 13 42 03 |
| Water-soluble, Cr ⁶⁺ | 0-2 | ppm | ≤ 2 | |

(In accordance with EG 2003/53 and KIFS 2004:6)

Appendix 2: XRD analysis of INJ30 and UF12

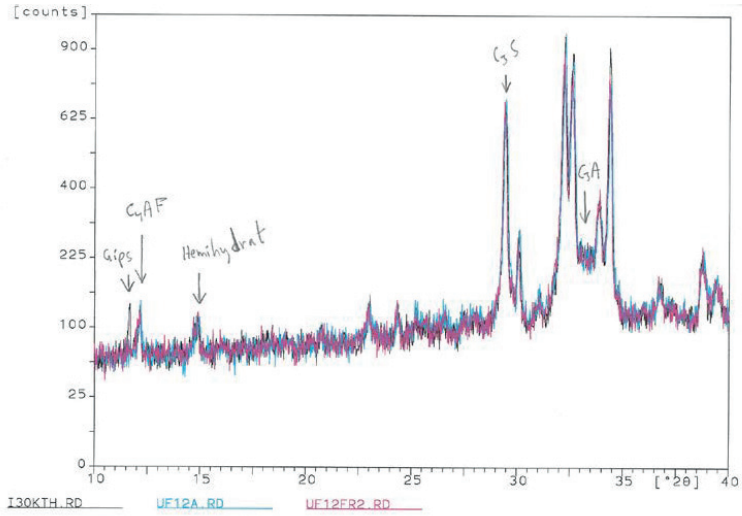


Figure 39: XRD analysis of unhydrated INJ, UF12 and modified UF12 cement

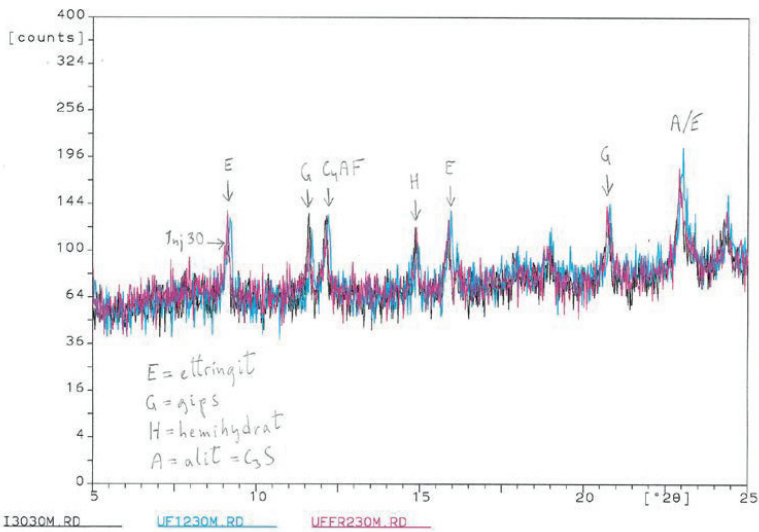


Figure 40: XRD analysis of hydrated INJ30, UF12, and modified UF12 cements after 30 minutes of hydration

Appendix 3: SEM analysis

Figure 41 shows an image of filter cake from INJ30 grout. The red rectangles show areas presented in the following figures. (Figure 42 - Figure 46). Figure 46 shows an area with a large concentration of fine material.

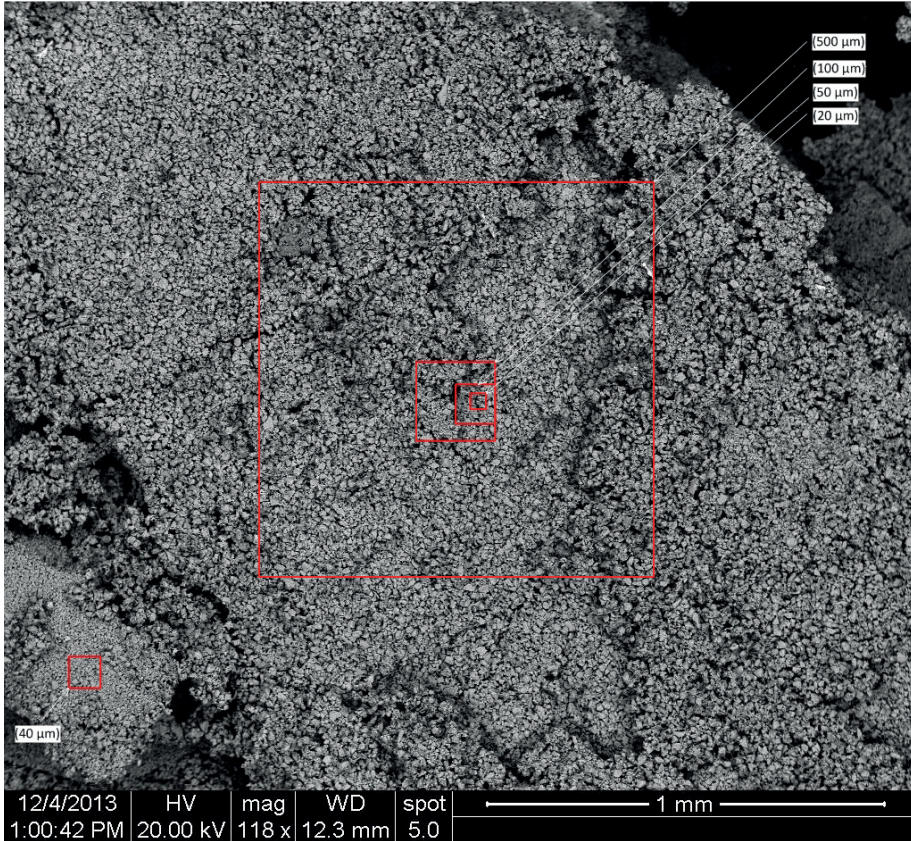


Figure 41: Image of filter cake from INJ30. Bar 1000 µm.

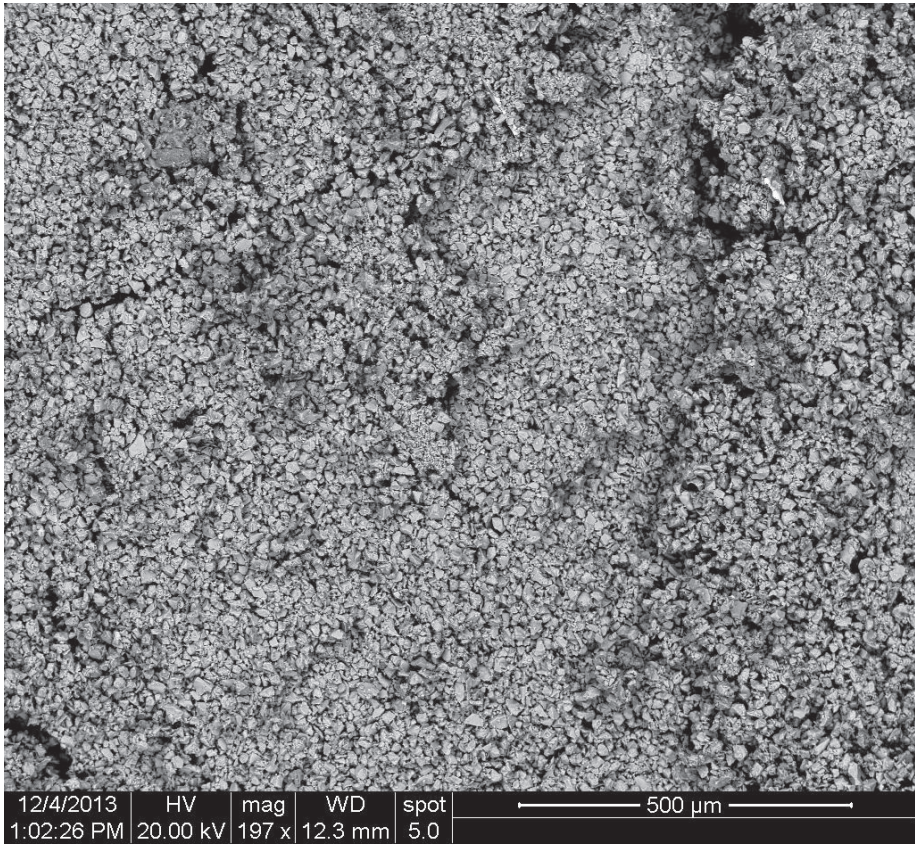


Figure 42: Image of filter cake from INJ30. Bar 500 μm.

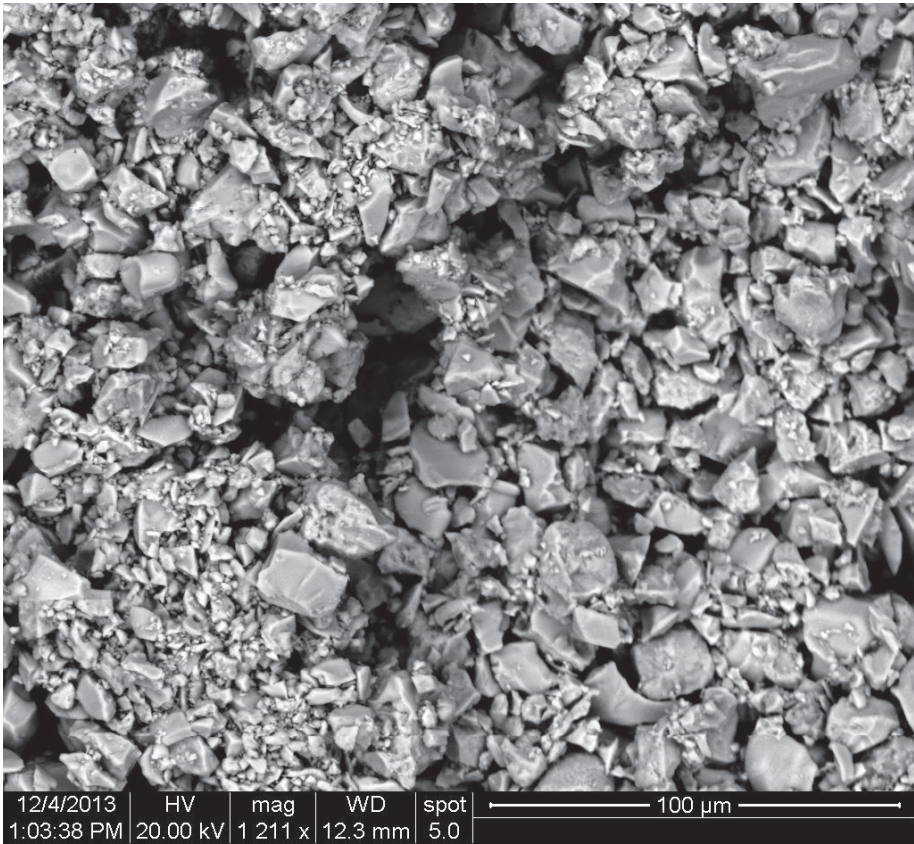


Figure 43: Image of filter cake from INJ30. Bar 100 µm.

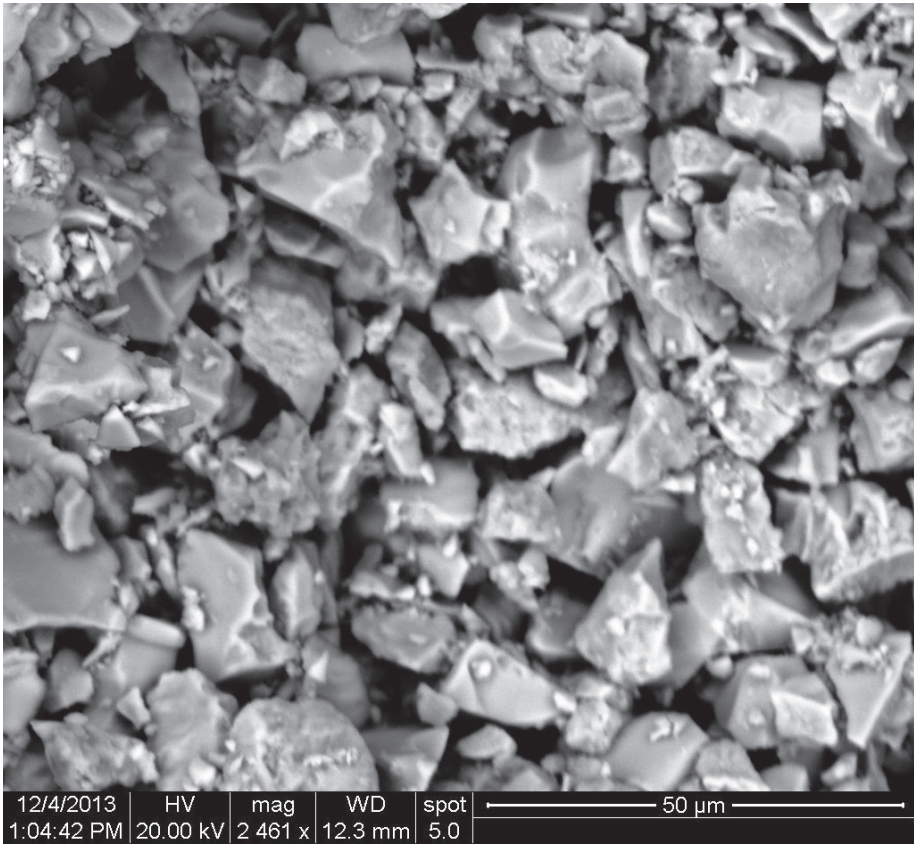


Figure 44: Image of filter cake from INJ30. Bar 50 µm.

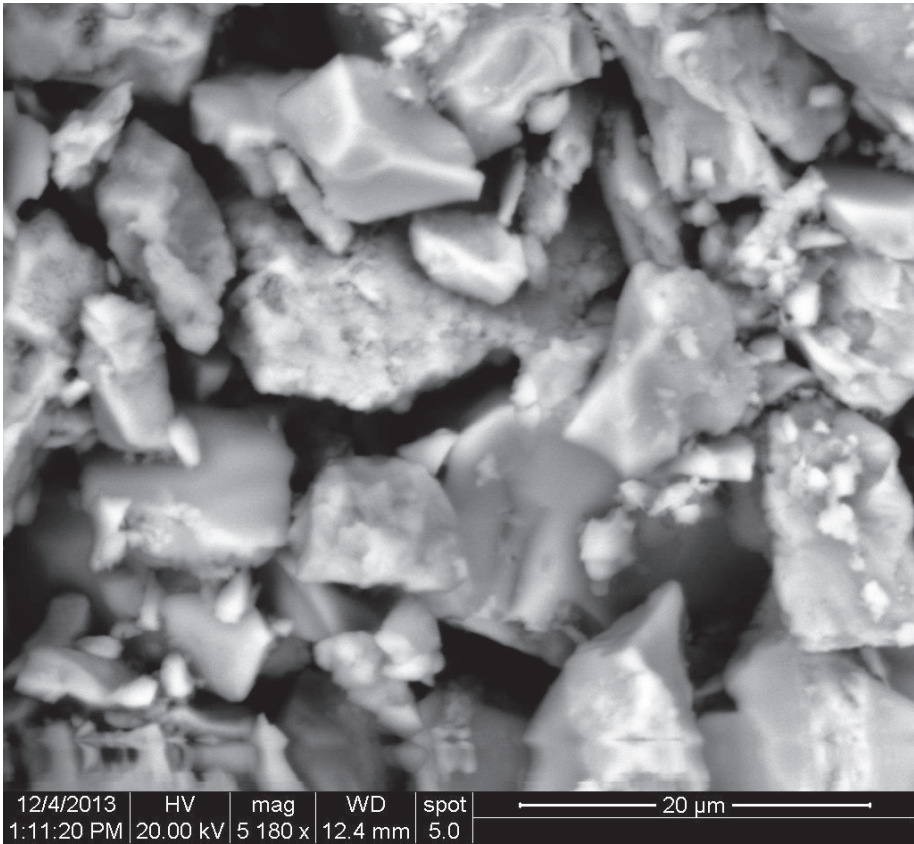


Figure 45: Image of filter cake from INJ30. Bar 20 µm.

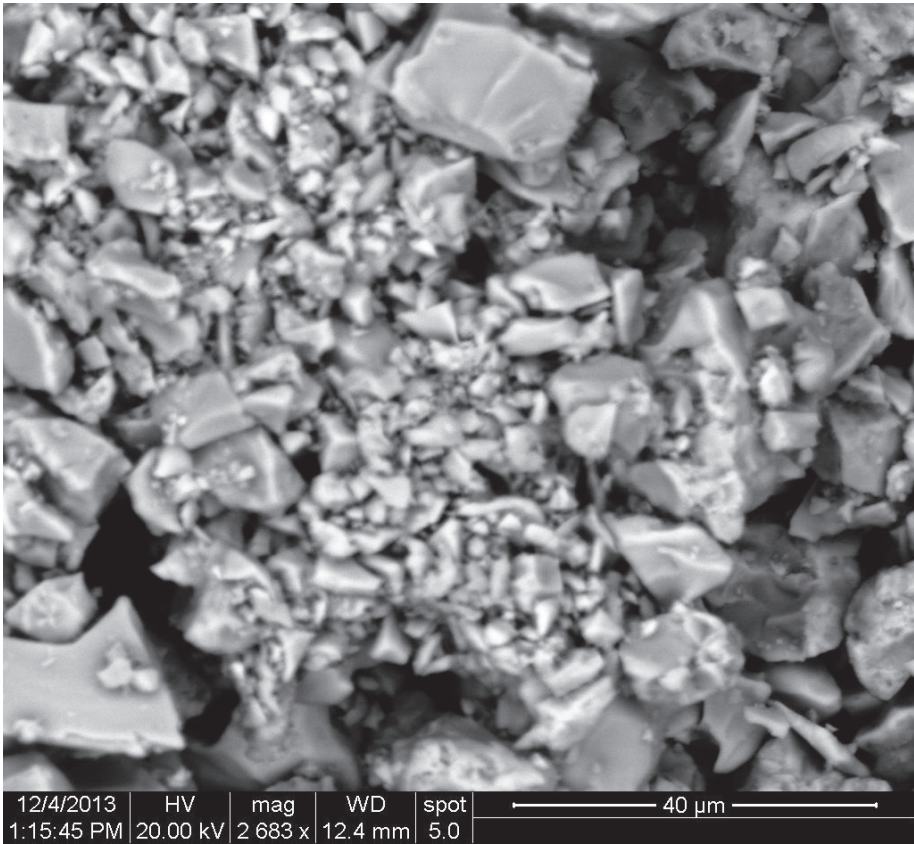


Figure 46: Image of filter cake from INJ30. Bar 40 µm. Assemblage of fine particles.

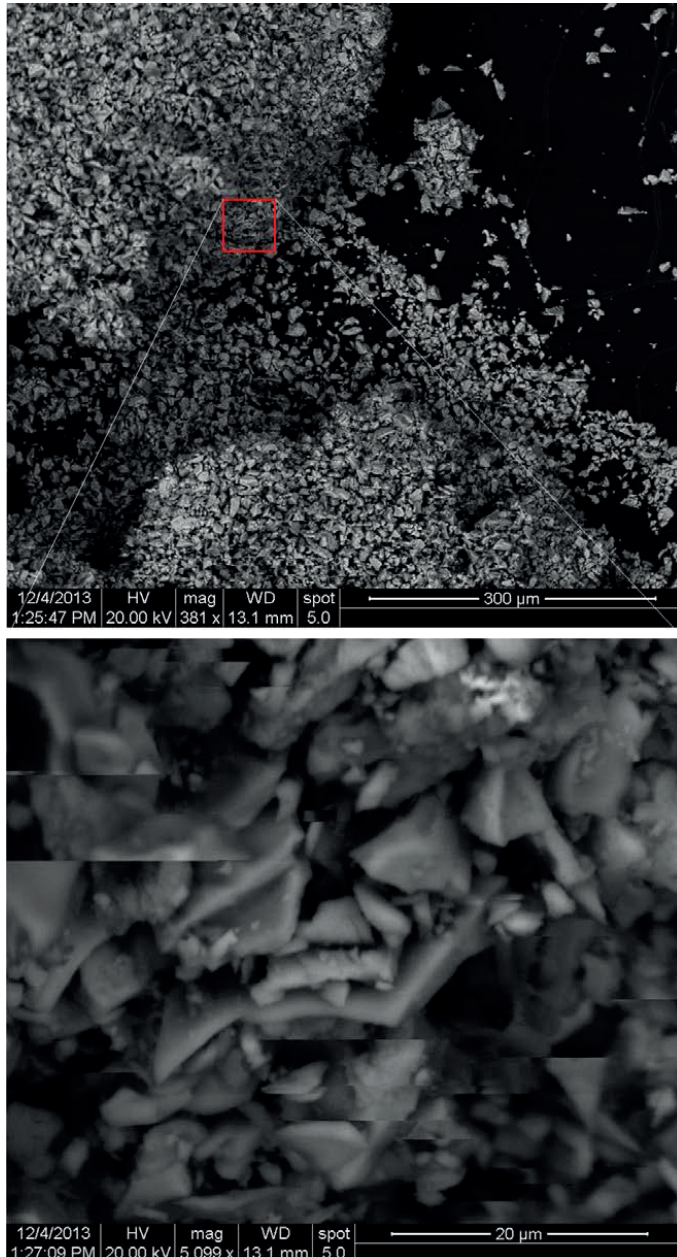


Figure 47: Image of filter cake from INJ30.



Box 5501
SE-114 85 Stockholm

info@befonline.org • www.befonline.org
Visiting address: Storgatan 19

ISSN 1104-1773